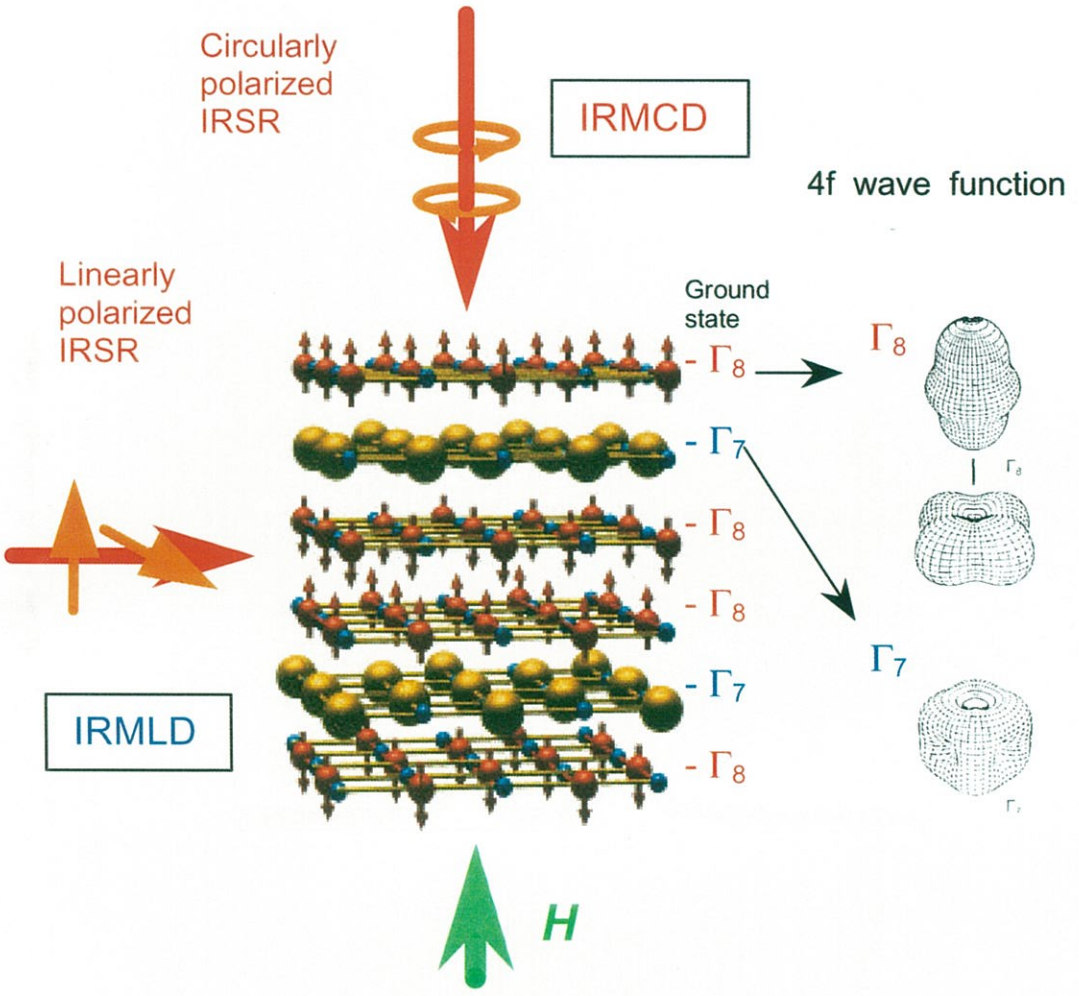

Solid State Spectroscopy I

(IR, VUV, etc)

BL1B, 3A1, 6A1, 7A, 7B

BL1B

LiCAF crystal as a new vacuum ultraviolet optical material with transmission down to 112 nm

M. Sakai[1], M. Kozeki[1], Z. Liu[1], H. Ohtake[1], N. Sarukura[1], Y. Miyazawa[2], K. Shimamura[3], S. L. Baldochi[3], K. Nakano[3], N. Mujilatu[3] and T. Fukuda[3]

[1] Institute for Molecular Science (IMS), Okazaki, Aichi 444-8585, Japan

[2] Research and Development Department, Optron Inc., Toride, Ibaraki 302-0032, Japan

[3] Institute for Materials Research, Tohoku University, Sendai, Miyagi 980-8577, Japan

Recently, various new fluoride crystals have been developed as the host crystals for new solid-state tunable ultraviolet and infrared laser materials. Ce:LiCAF and Ce:LiSAF are attractive solid-state lasers with their practical tuning region from 288 to 315 nm [1, 2]. To improve laser performance, further spectroscopic studies of these materials will be necessary, including accurate band-gap measurement of the host crystal. In addition, optical material for the ultraviolet and vacuum ultraviolet region has become much more important for the deep ultraviolet lithographic technology required for the semiconductor processing technology of the next century and vacuum ultraviolet spectroscopy using synchrotron orbital radiation.

Crystals of LiCAF, LiSAF and LiF were grown by the Czochralski method. The sample was about 1-mm thick. To measure the transmission edge of various fluoride materials at room temperature, an experiment was performed at Ultraviolet Synchrotron Orbital Radiation Facility (UVSOR). Figure 1, indicates the transmission spectrum of various fluoride samples. According this figure, transmission edge of LiCAF, LiSAF and LiF were 112 nm, 116 nm and 136 nm, respectively. From the transparent wavelength shorter than that of conventional LiF, the non hydroscopic nature of LiCAF, and the better mechanical properties compared with LiF, LiCAF is shown to be an ideal optical material for the vacuum ultraviolet region.

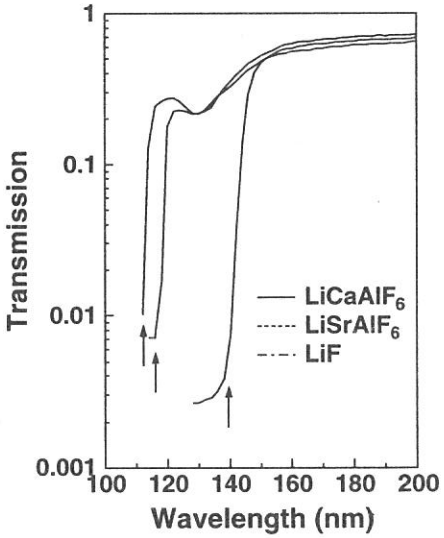

Fig. 1

The authors are grateful to Mr. M. Hasumoto, Dr. T. Gejo, and Prof. K. Kamada for their experimental support and stimulated discussion.

References

[1] See, for example, C. D. Marshall, S. A. Payne, J. A. Speth, W. F. Krupke, G. J. Quarles, V. Castillo and B. H. T. Chai: J. Opt. Soc. Am. B. **11** (1994) 2054-2057.

[2] See, for example, Z. Liu, S. Izumida, H. Ohtake, N. Sarukura, K. Shimamura, N. Mujilatu , S. L. Baldochi and T. Fukuda: Jpn. J. Appl. Phys., **37** (1998) L1318 –L1321

(BL1B)

Surface Excess of Dye Molecules at Gas/Water Interface Determined by Single-Photon Ionization Spectroscopy

Toshio Ishioka, Koichiro Seno, Shinya Sasaki, and Akira Harata

Department of Molecular and Material Sciences, Interdisciplinary Graduate School of Engineering Sciences, Kyushu University, Fukuoka, 816-8580 Japan

The understanding of molecular behavior at gas/water interface is of central importance in surface science, film technology, and environmental chemistry. For decades, they have been studied by methods such as surface tensiometry and radiochemical methods, yielding mostly information on the macroscopic level of interface. The recently developed nonlinear optical methods, such as second-harmonic generation (SHG), sum-frequency generation (SFG), and multi-photon ionization, have been providing essential information on microscopic molecular states of surfaces since they have specific sensitivity of 'just' interface. Though they are excellent in selectivity at interfaces, the mechanism of multi-photon process is usually complex and difficult to analyze quantitatively because resonant states often intervene in those processes. To solve above problem, we have tried to measure simple single-photon ionization spectra of dye molecule using synchrotron radiation, and compare the results with those of two-photon ionization and surface-tension measurements.

The experimental setup for single-photon ionization is shown in Fig. 1. Synchrotron photon-energy from 4.7 to 6.8 eV was used as an excitation source. The beam power was calibrated using a photomultiplier tube (Hamamatsu Photonics, R955) after each measurement. The beam was irradiated on the water surface containing various concentration of Rhodamine B (RhB). The solution was kept in a stainless-steel vessel so that high voltage was appliable between water surface and electron-trapping electrode settled in the gas. The photoionization current was measured using a current meter (Keithley, 617). Two-photon ionization experiment was carried out using third-harmonic (355 nm, 5 ns) of Nd:YAG laser (Minilite, Spectra Physics). Experimental configuration of two-photon ionization was approximately the same except for the excitation source and cell dimension. Surface tension was measured by a surface-pressure meter (Model HMB, Kyowakaimen, Japan) equipped with a glass plate of Wilhelmy type. RhB (reagent grade, Nacalaitesque, Japan) was used as received and dissolved into pure water. Water was purified until resistivity reached higher than 18 MΩcm by Milli-Q system (Milli-Q Academic, Millipore).

The normalized one-photon ionization spectra of RhB is shown as Fig. 2. All derived spectra obey a empirical 5/2 power law represented by

$$I = C\, E_{ex}^{2.5} = C\, (h\nu - E_{th})^{2.5} \qquad (1)$$

where E_{ex} is the excess energy of the ionized pair; C is the proportionality constant; and E_{th} is the ionization threshold. The abscissa in Fig. 2 should give the E_{th} value of eq.1. The derived threshold energy for RhB lies at 5.5–5.6 eV and does not depend on the bulk concentration, which would imply neither the chemical state of RhB nor the length from the surface are largely changed.

At fixed photon energy, the photoionization intensity should be linear with the number of photoionizing molecule at probe area. In Fig.2, the signal intensity at fixed photon energy above E_{th} monotonously increases with RhB concentration because surface density increase with bulk concentration. If linearity with surface concentration (which is equal to the thermodynamic definition of 'surface excess' when dilute solution is used) and photoionization intensity can be assumed, the adsorption isotherm can be discussed. In Fig. 3, the intensity of photoionization is plotted against bulk concentration, and obviously, it obeys Langmuir isotherm which was denoted by

$$\Gamma/(\Gamma_{max}-\Gamma) = \beta c \qquad (2)$$

where Γ and Γ_{max} denote surface excess and saturated surface excess, respectively; β is the adsorption parameter; and c is the bulk concentration of adsorbate. The result that RhB obey Langmuir isotherm is coincident with the result of two-photon ionization and surface tension measurement. Table 3 summarizes the result of adsorption parameter derived from these methods. They agree within a factor or two and show these methods are reliable to measure surface excess of RhB. Small deviation of each experimental value was, however, observed in Table 3, which may imply the difference of probe region (probe depth from surface) of these methods. Further discussion would be carried out in future articles.

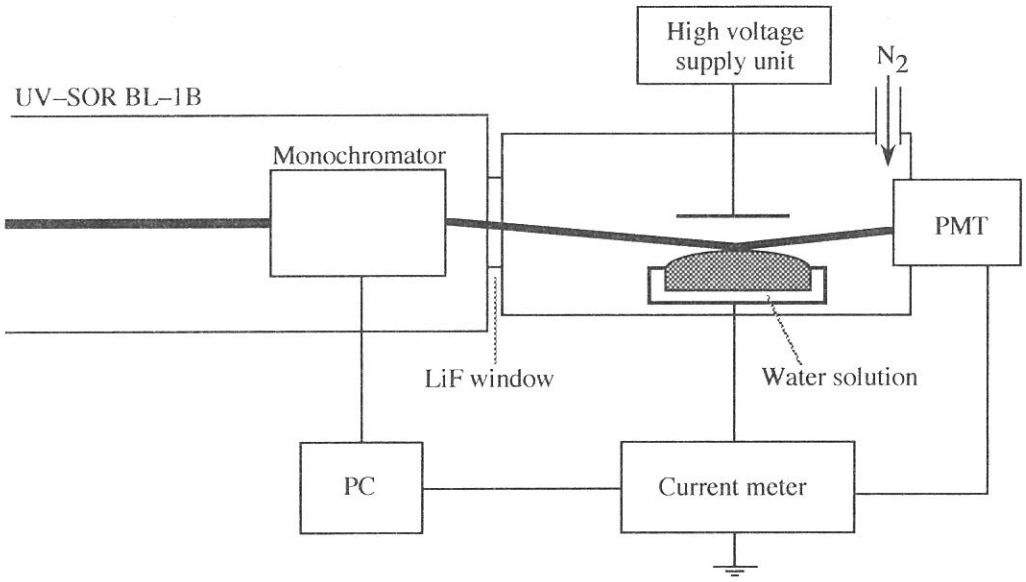

Fig. 1 Schematic diagram of the photoionization spectrometer using SOR light.

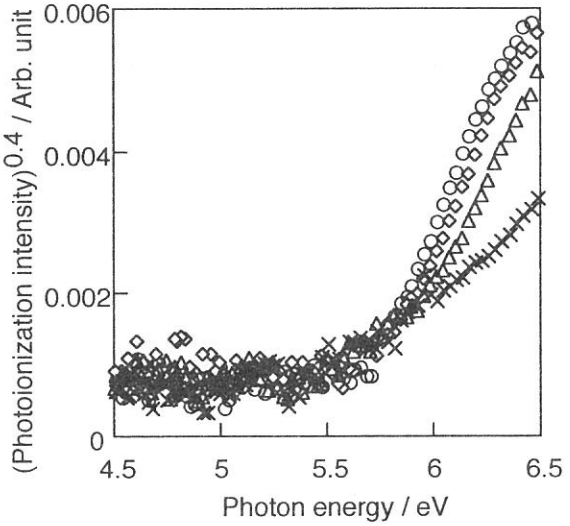

Fig. 2 Bulk concentration dependence of RhB on single-photon ionization spectra of water surface. Each RhB concentration was $1.0*10^{-4}$ M(circle), $1.0*10^{-5}$ M (lozenge), $2.0*10^{-6}$M (triangle), and $3.0*10^{-7}$ M (cross).

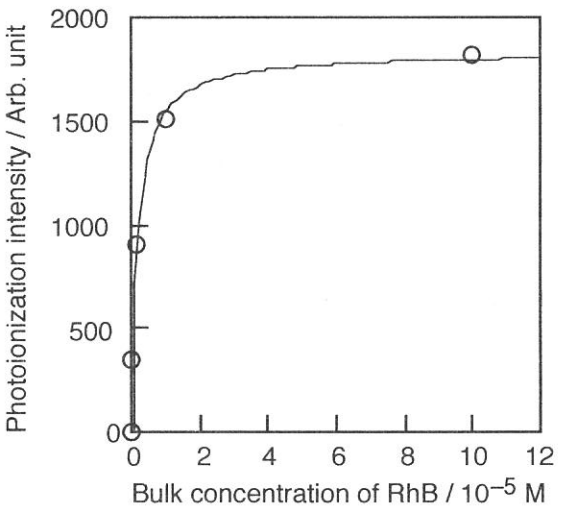

Fig. 3 Adsorption isotherm RhB onto water surface by single-photon ionization. The fitting was carried out using Langmuir isotherm.

Table 1 Adsorption parameter of RhB onto water derived by various methods.

Method	β / 10^5 mol^{-1} dm^3 *
single-photon ionization	5.2
two-photon ionization	3.9
surface tension	8.2

*) Langmuir isotherm: $\Gamma / (\Gamma_{sat}-\Gamma) = \beta a$; Γ(surface excess), Γ_{sat}(saturated surface excess), a (activity in bulk phase), β (adsorption parameter).

(BL1B) Reflection and luminescence spectra of $CaWO_4$ and $ZnWO_4$ crystals grown by flux method

Minoru ITOH, Michihiro HORIMOTO, Shuji OISHI[1] and Masami FUJITA[2]

Department of Electrical and Electronic Engineering, Shinshu University, Nagano 380-8553
[1] *Department of Environmental Science and Technology, Shinshu University, Nagano 380-8553*
[2] *Maritime Safety Academy, Wakaba, Kure 737-8512*

The second-group metal tungstate family has extensive applications and therefore has been intensively studied during the past half a century. However, there are still unanswered questions concerning the nature of the optical transitions; e.g., the importance of defects and impurities on the luminescence properties. Until now, all the crystals investigated have been grown from the melt by the Kyropoulos or Bridgman technique. This may introduce some local deformation due to thermal stress into the large-volume crystals. The growth method using flux has several principal advantages; the resultant crystals are relatively free of thermal stress and has a lower concentration of lattice imperfections, compared to the melt-grown crystals. In the present experiment, we have, for the first time, investigated the optical properties of $CaWO_4$ and $ZnWO_4$ crystals grown by the flux method. Calcium tungstate crystallizes in a scheelite (stolzite) structure, while zinc tungstate has a raspite (wolframite) structure.

Well-formed crystals of $CaWO_4$ were grown in Na_2WO_4 flux. The crystal growth was conducted by heating mixtures at 1100 °C for 5 h, followed by cooling to 500 °C at a rate of 5 °C/h [1]. Crystals of $ZnWO_4$ were prepared in Na_2O-WO_3 flux. The heating conditions for $ZnWO_4$ growth were almost the same as those in the case of $CaWO_4$ growth. Both crystals obtained were colorless and transparent, with flat surfaces. The X-ray diffraction indicated that our crystals of $CaWO_4$ and $ZnWO_4$ are single-phased.

A solid curve of Fig. 1 represents the reflection spectrum of $CaWO_4$ measured at 6 K under near-normal incidence configuration. There exist a sharp exciton band at 5.96 eV and a broad doublet structure in the spectral range between 8 and 12 eV. This spectrum is similar to the previous result obtained in ref. [2], although our doublet structure is larger in intensity than theirs. The reflection spectrum of $ZnWO_4$ is shown by a solid curve in Fig. 2. One can see a strong band peaking at 5.00 eV with sub-structures on the low- and high-energy sides, and a weak doublet structure in the 8－12 eV range. To our knowledge, there seems to be no reflection data of $ZnWO_4$ to be compared to our spectrum.

The $CaWO_4$ and $ZnWO_4$ emit a single luminescence peaking at 2.85 and 2.40 eV under excitation in the exciton-band region at 6 K, respectively. The spectra are shown in Fig. 3, where the collections were made for the dispersion of the analyzing monochromator and for the spectral response of the detection system. The excitation spectra for these two bands are shown by dotted curves in Figs. 1 and 2. It is evident that the 2.85- and 2.40-eV bands are an intrinsic feature to the respective systems, because they are stimulated with photons above the onset of the lowest exciton reflection bands. The 2.40-eV luminescence of $ZnWO_4$ exhibited two decay components at 6 K; fast one (1.2 ± 0.2 μs) and slow one (21 ± 1 μs). Decay measurement was not carried out for the 2.85-eV luminescence in $CaWO_4$. At 295 K, both emission bands are thermally quenched by 50%.

When $CaWO_4$ is excited around 4.6 eV on the low-energy side of the exciton band, two weak emission bands appear at about 2.45 and 2.70 eV. They are most likely due to lattice imperfections. On the other hand, no other luminescence was observed in $ZnWO_4$.

According to a recent band structure calculation of some tungstate crystals [3], the main exciton peaks in Figs. 1 and 2 would be ascribed to the optical transitions from the O 2*p* states to the W 5*d* states. It is, therefore, supposed that the 2.85-eV emission band of $CaWO_4$ arises from radiative annihilation of excitons self-trapped on WO_4 molecular groups in which four oxygen ions form the tetrahedron with a tungsten ion at the center. On the other hand, the emission band at 2.40 eV in $ZnWO_4$ is attributed to excitons self-trapped on octahedral WO_6 groups in which a tungsten ion is surrounded by six oxygen ions. The luminescence in monoclinic tungstate crystals of raspite-type appears at the energy lower than that in tetragonal ones of scheelite-type. This general trend has nicely been confirmed for $PbWO_4$ by our recent experiment [4].

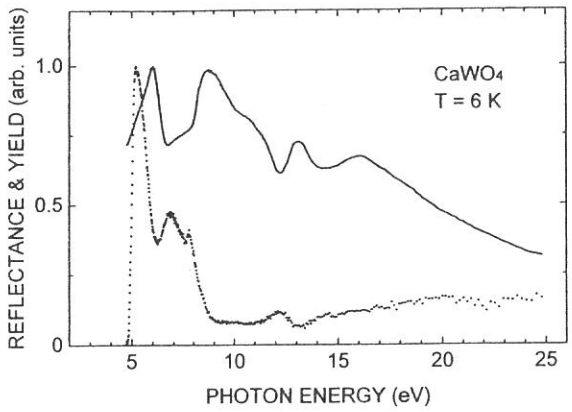

Fig. 1. $CaWO_4$: reflection spectrum (solid curve) and excitation spectrum (dotted curve) for the 2.85-eV band.

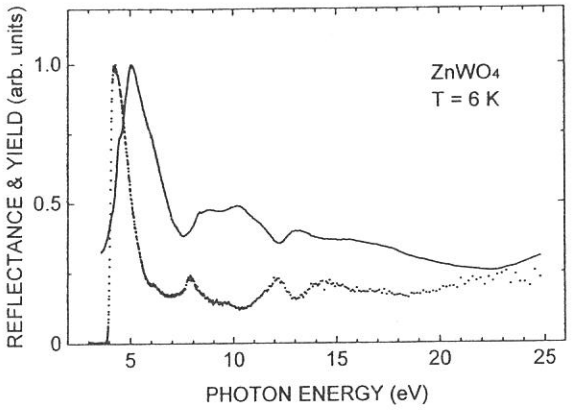

Fig. 2. $ZnWO_4$: reflection spectrum (solid curve) and excitation spectrum (dotted curve) for the 2.40-eV band.

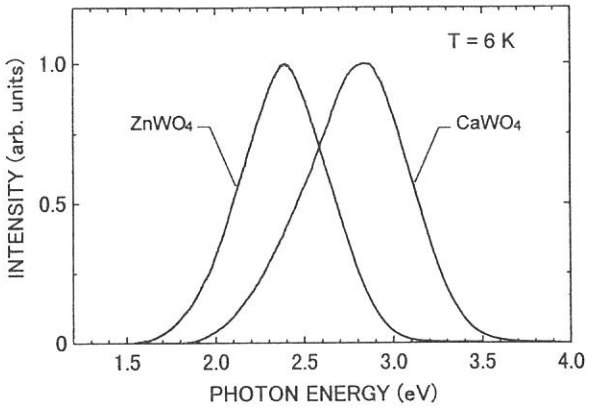

Fig. 3. Luminescence spectra of $CaWO_4$ and $ZnWO_4$ excited at 6 K with 5.15- and 4.45-eV photons, respectively.

[1] S. Oishi and M. Hirao: Bull. Chem. Soc. Jpn. **63** (1990) 2721.

[2] R. Grasser, E. Pitt, A. Scharmann and G. Zimmerer: Phys. Status Solidi (B) **69** (1975) 359.

[3] Y. Zhang, N. A. W. Holzwarth and R. T. Williams: Phys Rev. B **57** (1998) 12738.

[4] M. Itoh, D. L. Alov and M. Fujita: J. Lumin. (in press).

(BL1B)

Photoluminescence in amorphous silicon oxynitride grown by plasma-enhanced chemical vapor deposition

Hiromitsu *KATO*, Kwang Soo *SEOL**, Makoto *FUJIMAKI***, Takashi *NOMA****, Takashi *WATANABE*, and Yoshimichi *OHKI*
Department of Electrical, Electronics, and Computer Engineering,
Waseda University, Shinjuku-ku, Tokyo 169-8555.
* Applied Laser Chemistry Lab., RIKEN (The Institute of Physical and Chemical Research),
Hirosawa, Wako-shi, Saitama 351-0198.
** Research Fellow of the Japan Society for the Promotion of Science.
***Engineering Department 1, MOS-LSI Division, Semiconductor Company, Sanyo Electric Co. Ltd,
Oizumi-Machi, Gumma 370-0596.

Category 4. Solid- & liquid-phase spectroscopy 1 (IR, VUV, etc)

I. EXPERIMENTAL PROCEDURES

The amorphous silicon oxynitride (a-SiO_xN_y) films were deposited on a silicon monocrystal substrate by plasma enhanced chemical vapor deposition at a substrate temperature of 400 °C using SiH_4, N_2O and N_2 as monomer gases. The thickness of these films was about 100 nm. By changing the flow rate of SiH_4, samples A to E shown in Table I were obtained. The ratio of y/x was measured using X-ray photoelectron spectroscopy (JEOL JPS-90MX). Photoluminescence (PL) spectra, PL excitation (PLE) spectra and PL decay profiles were measured using synchrotron radiation (SR) at BL1B line in UVSOR. The PL and PLE spectra were measured under multi bunch operation mode at 14 K, and the PL decay profiles were measured at 14 K by a time-correlated single photon counting technique under single-bunch operation mode.

II. RESULTS AND DISCUSSION

Figure 1 (a) shows the PL spectrum of sample B excited by 5.0 eV photons. Intense PL is observed at 4.4 eV. Figure (b) shows the PLE spectrum of the 4.4 eV band. As shown in Fig.1 (b), the 4.4 eV band has two PLE bands at 5.0 eV and 7.3 eV. Figure 2 shows decay profiles of the 4.4eV band excited at 5.0 eV (a) and 7.3 eV (b). The data were fitted by the least-squares method with the time derivative of a stretched exponential function,

$$I(t) \propto (\beta/\tau)(\tau/t)^{1-\beta}\exp(-(t/\tau)^{\beta}). \qquad (1)$$

Here, τ and β are the effective lifetime and a parameter which takes a value of $0<\beta<1$, respectively. This is consistent with many reports which revealed that the luminescence decay in many amorphous materials is described by the above equation. The lifetime of the 4.4 eV band is 3.4 ns under the 5.0 eV excitation and is 2.2 ns under the 7.3 eV excitation. These values agree well with the ones reported for the lifetime of 4.4 eV band due to the oxygen vacancy (≡Si-Si≡, '≡' denotes bonds with three separate oxygen atoms) in the oxygen-deficient-type bulk SiO_2. The 4.4 eV band in SiO_2 is considered to be due to an electronic transition from the excited singlet state to the ground state. The oxygen vacancy in SiO_2 also gives rise to a PL band at 2.7 eV, which is due to an electronic transition from the excited triplet state to the ground state. Since this 2.7 eV band involves a thermally activated intersystem crossing, its intensity decreases as the temperature decreases. These characteristics, namely, the concurrence of two PLs at 2.7 and 4.4 eV, the PLE spectrum and the lifetime of the 4.4 eV band, and the temperature dependence of the 2.7 eV band agree quite well with those of the PL bands shown in Fig.1. This indicates that sample B includes oxygen-deficient SiO_2.

Figure 3 shows the PL spectrum (a) of sample E excited at 5.0 eV and the PLE spectrum (b) monitored at 2.6 eV. The 4.4 eV band does not appear, indicating that the oxygen-deficient SiO_2 was not present. For comparison, the PL and PLE spectra are also shown for hydrogenated amorphous silicon nitride (a-SiN_x:H) deposited by low-pressure chemical vapor deposition. In both samples, the 2.6 eV band is seen. From Fig.3 (b), it is considered that both the 2.6 eV band in sample E and the 2.6 eV band in SiN_x are excited by interband photon absorption. The subtle difference in the photon energy at which the PLE spectrum starts to rise is presumably due to the difference in the optical absorption edge in the two materials. The lifetime τ is 3.2 ns for sample E and 3.7 ns for SiN_x, while β is 0.39 and 0.40. This good agreement indicates that the two PLs are caused by the same mechanism. The 2.6 eV band of SiN_x is considered to be related to recombination of electrons and holes, generated by interband photon absorption. It is therefore considered that the 2.6 eV band in sample E is caused by the same mechanism, and that sample E includes, at least partially, the structure of SiN_x.

As a function of y/x, the change of the two PL intensities, 2.6 eV and 4.4 eV, clearly shows that the contribution of PL from SiN_x is weak if y/x is small and becomes stronger when y/x becomes larger. This indicates that the present samples, SiO_xN_y, are not a perfect compound, and includes, at least partially, SiO_2 and SiN_x. The ratio of SiN_x and SiO_2 depends primarily on the ratio y/x.

Table I. The y/x ratio and refractive index for SiO_xN_y films examined.

Sample	y/x	refractive index
A	0.054	1.49
B	0.112	1.52
C	0.125	1.54
D	0.148	1.56
E	0.161	1.59

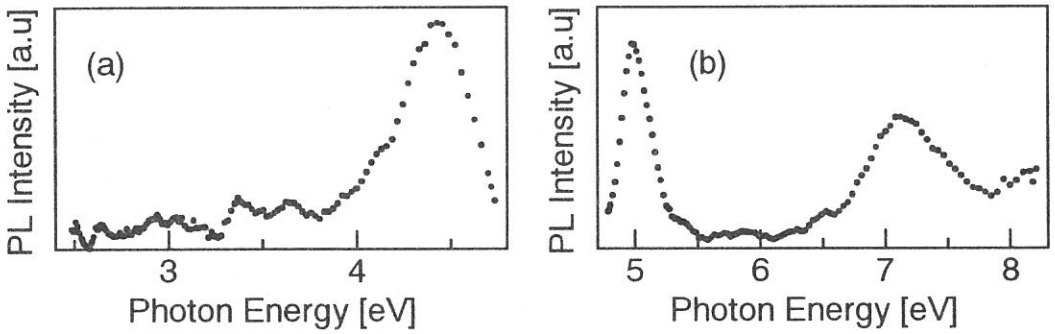

FIG.1. PL spectrum (a) of sample B at 14 K excited by 5.0 eV photons and PLE spectrum (b) of the 4.4 eV band.

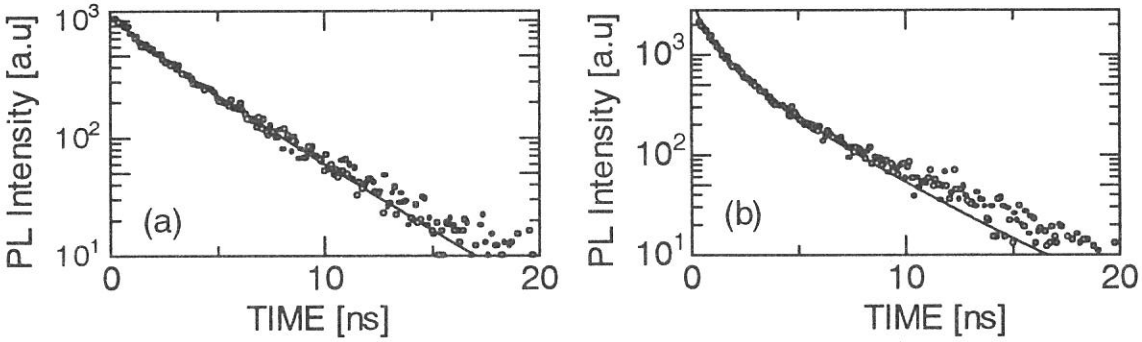

FIG.2. Decay profiles of the 4.4 eV band excited at 5.0 eV (a) and 7.3 eV (b) for sample B. Solid curves are drawn by assuming the stretched exponential function, Eq. (1).

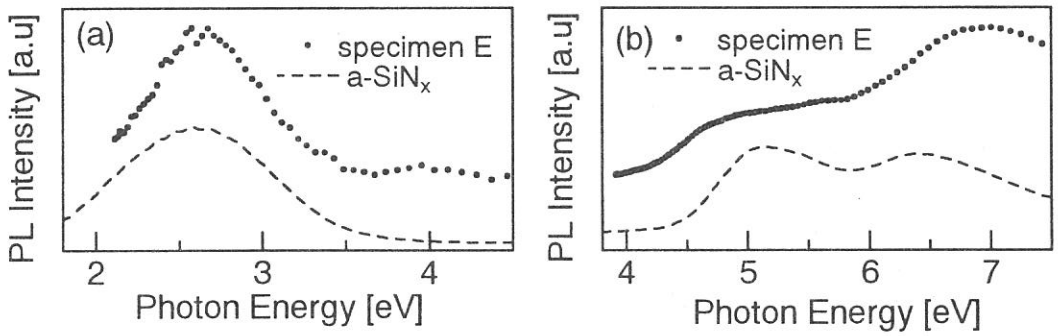

FIG.3. PL spectrum excited by 5.0 eV photons (a) and PLE spectrum of the 2.6 eV PL band (b) for sample E (solid curves) and SiN_x (broken curves).

(BL1B)

Reflection Spectra of Hydrogen-Bonded Ferroelectric $PbDPO_4$

Noriaki KIDA, Nobuhito OHNO[A], Yoshihiko YAMAZAKI[A] and Masao KAMADA[B]

Research Center for Superconducting Materials and Electronics, Osaka University, Suita, Osaka 565-0871, Japan
[A] Division of Electronics and Applied Physics, Graduate School of Engineering, Osaka Electro-Communication University, Neyagawa, Osaka 572-8530, Japan
[B] UVSOR Facility, Institute for Molecular Science, Okazaki, Aichi 444-8585, Japan

Lead monohydrogen phosphate $PbHPO_4$ (LHP) is a hydrogen-bonded ferroelectric material. It shows a second-order structural phase transition from a monoclinic Pc to a paraelectric $P2/c$ at T_C=310 K. The PO_4 tetrahedra are linked to linear chains by short O-H-O bonds and not cross-linked to one another, in contrast to well studied KH_2PO_4 (KDP) [1]. Therefore, LHP and its isomorphic compounds are regarded as quasi-one dimensional ferroelectrics. The most famous phenomenon of the hydrogen-bondend ferroelectric materials is the isotope effect — Curie point T_C corresponding to the onset temperature of ferroelectric order increases by substituting deuterium for hydrogen atoms —. In deuterium compound of LHP, $PbDPO_4$ (DLHP), T_C increases to about 450 K [2].

Up to now, optical response of LHP and $PbHAsO_4$ (LHA) has been investigated [3]. The clear direct excitonic transitions are observed at the fundamental absorption edge. These transitions are assigned due to intra-cationic Pb^{2+} transitions ($6s \rightarrow 6p$). The Urbach rule holds well for the absorption edge of LHP. The conversing energy is found to be different between ferro- and paraelectric phases. The temperature profile of the steepness parameter (σ) of LHP derived from Urbach slope exhibits an anomalous behavior. Moreover, the observed temperature-dependent σ is well scaled to that of the spontaneous polarization (P_S) with the scaling factor $\sim 1/2$. Recently, Noba and Kayanuma have theoretically shown that excitons in the ferroelectric phase are strongly affected by the Stark effects induced by the local fields due to the hydrogen ordering [4]. It is interesting to study the optical properties of DLHP, to see the isotope effect on the electronic structure of LHP.

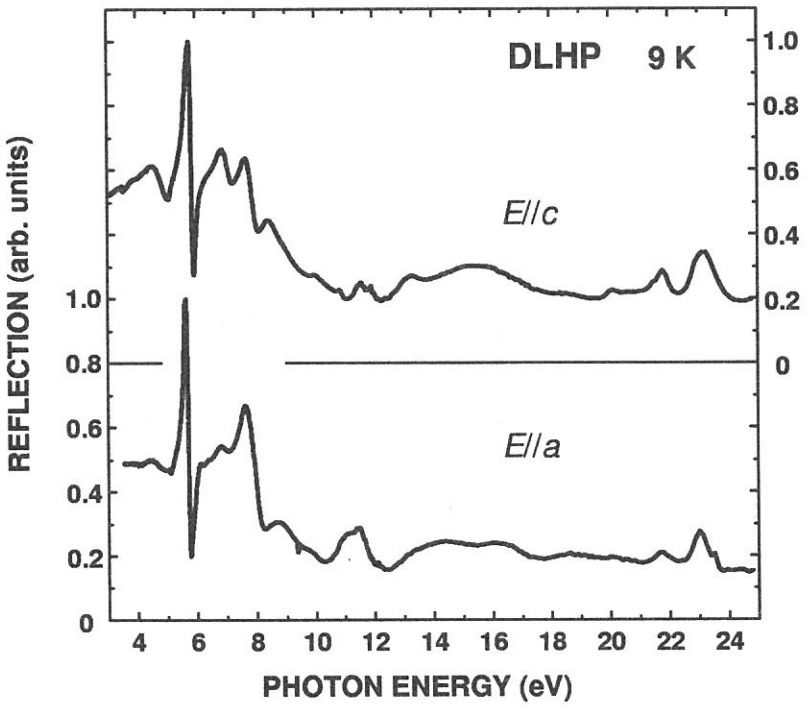

Figure 1: Polarized reflection spectra of DLHP for $E//a$ (lower) and $E//c$ (upper) at 9 K. Each spectrum is normalized at maximum.

Table 1: The first direct exciton transition energy E_1, the exciton binding energy E_B and the band-gap energy E_G for DLHP and LHP ($E//a$).

	E_1 (eV)	E_B (eV)	E_G (eV)
DLHP	5.63	0.67	6.30
LHP	5.62	0.67	6.29

In the present investigations, reflection spectra of a single crystal of DLHP have been investigated for the first time in the VUV region up to 25 eV by using polarized synchrotron radiation at the BL1B beamline. The specimens of DLHP grown from the conventional gel-growth method were used for optical measurements.

Figure 1 shows the reflection spectra of a single crystal of DLHP for polarization parallel to the crystallographic a-axis ($E//a$) and the c-axis ($E//c$), respectively, measured at 9 K. The direction of P_S is in the ac plain, nearly close to the a-axis. Distinguished sharp peaks with dispersive structure are observed at the absorption edge at 5.63 eV for $E//a$ and at 5.77 eV for $E//c$. In LHP, these structures are located at 5.62 eV for $E//a$ and at 5.77 eV for $E//c$. These transitions have been ascribed to the cationic transition Pb^{2+} ($6s \rightarrow 6p$) based on the comparative results of the isomorphic compound LHA as well as KDP [3]. Hence, the first excitonic bands in DLHP are assigned as cationic-intraband transition of Pb^{2+} ions as in LHP. With increasing temperature, these structures shift to the lower energy side. They are clearly seen even at room temperature. This fact indicates that the exciton has a large binding energy (E_B).

A clear shoulder structure is observed on the higher energy side of the first direct exciton transition for $E//a$ at 6.13 eV. This transition peak is assigned to the n=2 state of exciton Rydberg series. We adopt the hydrogen-like energy model and estimate E_B and the band-gap energy (E_G) of DLHP as summarized in Table 1 together with LHP.

Spectral profile and peak energy positions are resemble to those of LHP. These results suggest that the electronic state of exciton is not affected by the *statical* hydrogen atoms. Hence the change of σ with temperature as observed in LHP is responsible for the *dynamics* of surrounding atoms.

The structures around 22 eV are attributed to the Pb^{2+} $5d \rightarrow 6p$ core excitons. Sharp peaks at 21.7 eV and 23.0 eV for $E//a$ are assigned to the transitions from the $^1S_0$ state to the $^3P_1$ and $^1P_1$ excited states, as in the cases of LHP and lead halides [3, 5]. As compared with LHP and LHA, these structures are more clearly seen in DLHP. An additional structure on the higher energy at 23.5 eV for $E//a$ is probably due to the transition to the $^3D_1$ state.

We thank Dr. D. J. Lockwood for kindly providing single crystals of DLHP.

References

[1] F. Jona and G. Shirane, Ferroelectric Crystals, p63 (Dover, United States, 1993).

[2] K. Deguchi and E. Nakamura, J. Phys. Soc. Jpn. **57**, 413 (1988).

[3] N. Kida, N. Ohno, K. Deguchi, and M. Kamada, J. Electron Spectrosc. Relat. Phenom. **101-103**, 603 (1999); N. Ohno and N. Kida, Ferroelectrics **223**, 389 (1999); N. Kida, Bussei Kenkyu (Kyoto) **63**, 477 (1999) [in Japanese]; N. Kida, N. Ohno, and M. Kamada, UVSOR Activity Report **1998**, 86 (1999).

[4] K. Noba and Y. Kayanuma, Phys. Rev. B **60**, 4418 (1999).

[5] M. Fujita, H. Nakagawa, K. Fukui, H. Matsumoto, T. Miyanaga, and M. Watanabe, J. Phys. Soc. Jpn. **60**, 4983 (1991).

(BL-1B)

Multiplication process of free excitons in $CsPbCl_3$ crystal

Mamoru KITAURA and Akimasa OHNISHI[A]

Fukui National College of Technology, Sabae 916-8507

[A]*Department of Physics, Yamagata University, Yamagata 990-8560*

Excitation spectra for luminescence in the energy region exceeding the band-gap energy by several times are know to contain information on multiplication process of electronic excitations (EE's). [1] In the present work, we measured the excitation spectrum for the free exciton luminescence in $CsPbCl_3$ crystals at BL-1B beam line of UVSOR and investigated the multiplication process of EE's in this material.

$CsPbCl_3$ single crystals were grown from melt in sealed quartz ampoules by the Bridgman method. The crystal samples were mounted on a Cu holder of a liquid helium cryostat and were cooled down to 15 K by thermal conduction. The free exciton luminescence was detected with a photomultiplier (Hamamatsu R955) through a grating monochromator (Jobin-Yvon HR320). The excitation spectra measured were corrected for both the spectral distribution and reflection losses of an excitation light.

Figure 1 shows the excitation spectrum for the free exciton luminescence of $CsPbCl_3$ at 15 K. For reference, the reflection spectrum at 15 K is also shown by a broken line. In spite of the correction for reflection losses of an excitation light, the excitation spectrum for the free exciton luminescence exhibits dips at reflection peaks. The dips should be connected to nonradiative annihilation of EE's at the crystal surface, because optical excitation at the reflection peaks with high absorption coefficient creates high concentrated EE's at the crystal surface.

The free exciton luminescence is excited with photons in the whole absorption region. It drastically increases its intensity in the energy range of 9.5-12.5 eV, and reaches almost twice that at 9 eV where one photon creates one *e-h* pair. Such increase in the intensity of the free exciton luminescence takes place beyond three times the band gap energy. These results undoubtedly satisfy a condition for multiplication processes of EE's. Heiderich *et al.* [2] measured the reflection spectrum of $CsPbCl_3$ and assigned reflection structures between 8 and 10 eV to electronic transitions from the VB of Cl 3*p* states to higher lying Cs 6*s* conduction states. Furthermore, they calculated its energy band structure and presented that the Cs 6*s* conduction states lie above the conduction band (CB) bottom of Pb 6*p* orbitals by 2.9 eV. It is worth noting that the energy between the Cs 6*s* and the Pb 6*p* states is almost equal to that of the lowest exciton peak. On this basis, the following situation will be supposed for the increase in the free exciton luminescence intensity in the 9.5 - 12.5 eV range. Hot photoelectrons optically created in the Cs 6*s* conduction states will release their kinetic energies through an inelastic scattering on valence electrons, and then relax into the conduction band bottom. The released kinetic energies are transferred to cause secondary excitation of the valence electrons. As a result, a free exction is secondarily produced besides an initially created *e-h* pair. The production of a free exciton

and an *e-h* pair results in the twice value of the free exciton luminescence intensity at 12.5 eV. Therefore, we attribute the increase in the 9.5 - 12.5 eV range to secondary formation of free excitons due to an inelastic scattering of hot photoelectrons in the Cs 6*s* conduction states on valence electrons.

In the 12.5 - 15 eV range, the free exciton luminescence is slightly enhanced. Since this energy range includes contribution of electronic transitions from Cs 5*p* core levels to the CB [2], such a slight enhancement in the free exciton luminescence originates from creation of Cs 5*p* core holes. From ref. 2, the energy between the top of the Cs 5*p* levels and the bottom of the VB is estimated to be about 3 eV. This value is almost equal to the band-gap energy and is enough to excite valence electrons into the CB bottom. It is thus possible to generate secondary valence excitation, when the Cs 5*p* core holes combine with valence electrons to decay nonradiatively. Therefore, we attribute the enhancement in the 12.5 - 15 eV range to secondary formation of *e-h* pairs accompanied by nonradiative decay of a photohole in the Cs 5*p* core levels.

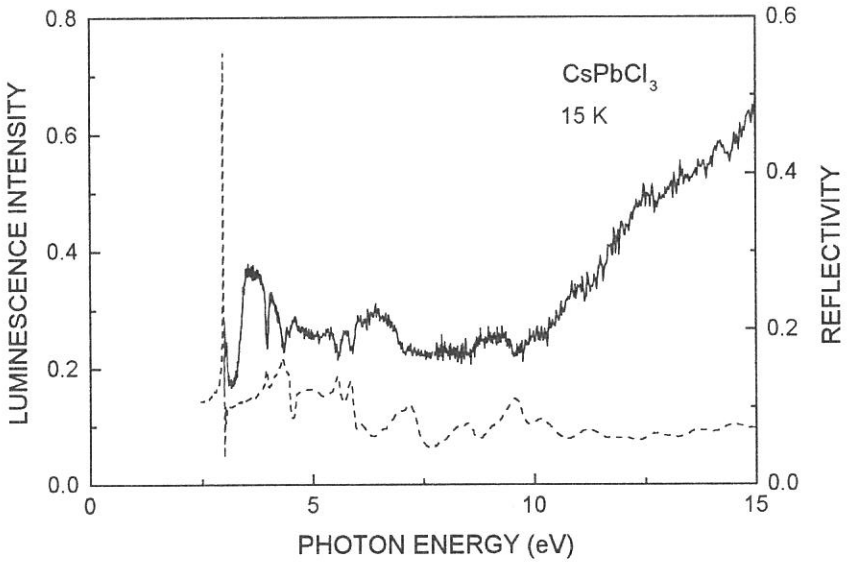

Fig. 1: Excitation spectrum for the free exciton luminescence line of $CsPbCl_3$ observed at 15 K. For reference, the reflectivity spectrum at 15 K is shown by a broken curve.

References

[1] A. Lushchik, E. Ferdbach, R. Kink and Ch. Lushchik: Phys. Rev. B, **53** (1996) 5379.

[2] K. Heidrich, W. Schafer, M. Schreiber, J. Sochtig, G. Trendel and J. Treusch: Phys. Rev. B, **24** (1981) 5642.

(BL-1B)

Reflection Spectra of $(C_2H_5NH_3)_2CdCl_4$ Single Crystal

Akimasa OHNISHI, Ken-ichi TANAKA, Takafumi OTOMO,
Takehisa YOSHINARI and Mamoru Kitaura[A]
Department of Physics, Yamagata University, Yamagata 990-8560
[A]*Fukui Department of Physics and Mathematics, National College of Technology, Sabae 916-8507*

We have studied the lowest exciton absorption of $(C_2H_5NH_3)_2CdCl_4$ single crystal and reported that the upper valence band (VB) and the lowest conduction band (CB) are constructed from the Cl 3*p* and Cd 5*s* states, respectively.[1] In the present work, we measured the optical reflection spectra of $(C_2H_5NH_3)_2CdCl_4$ up to 30 eV and investigated the energy band structure and the nature of optical transitions.

$(C_2H_5NH_3)_2CdCl_4$ single crystals were grown by slow evaporation method from the aqueous solution of $C_2H_5NH_3Cl$ and $CdCl_2$ at room temperature in dark. The measurements of reflection spectra for the polarization perpendicular to the *c*-axis (E ⊥ c) were carried out at BL-1B of UVSOR equipped with a 1m Seya-Namioka type monochromator. The spectral distribution of the incident light and the reflection light from the sample crystals was detected by a photomultiplier (Hamamatsu R105) coated with sodium salicylate, which is placed inside the sample chamber.

Figure 1 shows the reflection spectrum of the cleaved surface of $(C_2H_5NH_3)_2CdCl_4$ at 7 K in the range of 3 - 30 eV for the polarization E ⊥ c. The reflection spectrum is more refined than the previous report.[2] A sharp peak (X_1) is observed at 6.20 eV with an additional structure (X_2) appearing as the shoulder at 6.35 eV. The energy difference between the structures X_1 and X_2 is 0.15 eV and is comparable with the spin-orbit splitting energy of a Cl atom. Further, the peak energies of the structures X_1 and X_2 are almost same as the 1*s* exciton peaks of $CdCl_2$.[3] Thus, we attribute the structures X_1 and X_2 to the excitonic transition from the Cl 3*p* VB to the Cd 5*s* CB. A small hump (X_3) is observed at 6.97 eV. This hump may be due to the n = 2 exciton series of $(C_2H_5NH_3)_2CdCl_4$. A sharp peak (A) is also observed at 8.19 eV.

Figure 2 shows temperature dependence of reflection spectra (E ⊥ c) of $(C_2H_5NH_3)_2CdCl_4$ in the range of 5 - 10 eV. The reflection spectra were measured at temperatures of 7 - 280 K. Up on raising the temperature from 7 K, the X_1 peak at 6.20 eV shifts continuously to the low energy side, as indicated by a line. On the other hand, the peak A at 8.19 eV indicates the discontinuous low-energy-shift by 0.1 eV between 190 K and 220 K, as indicated by another lines. Such a discontinuous peak-shift is most likely caused by the structural phase transition taking place at 216.2 K in $(C_2H_5NH_3)_2CdCl_4$.[4] When the phase transition occurs, the relative arrangement between the NH_3 heads and the adjoining Cl ions largely changes, while that between the Cd ions and the Cl ions hardly changes. On the analogy of NH_4Cl crystal in which the NH_4 ions form the *s*-like CB,[5] we suppose that the peak A at 8.19 eV originates from the electronic transition from the Cl 3*p* VB to the second CB constructed from the *s*-like states of NH_3 heads.

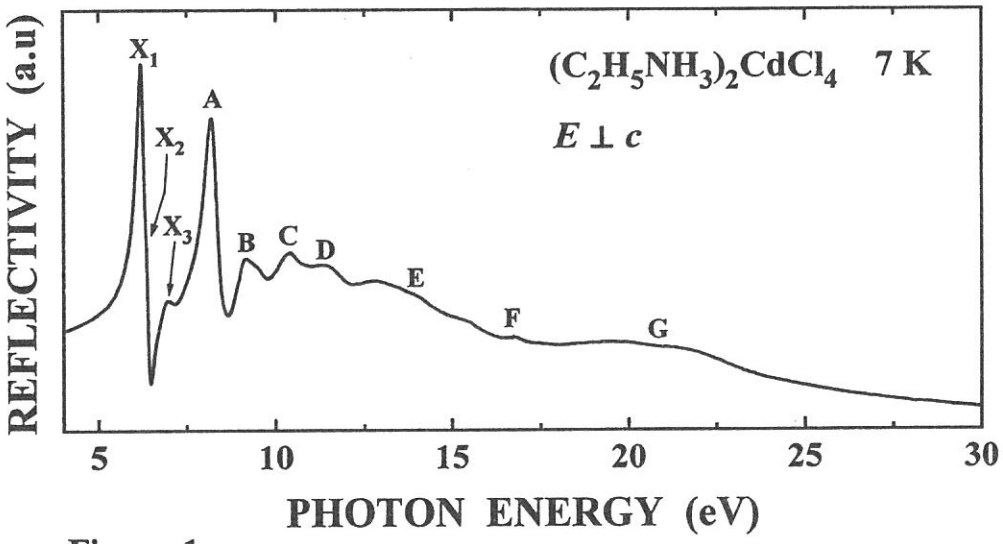

Figure 1

References

1)A. Ohnishi, K. Tanaka and T. Yoshinari: J. Phys. Soc. Jpn. **68** (1999) 288.

2)T. Yoshinari, T. Nanba, S. Shimanuki, M. Fujisawa, T. Matsuyama, M. Ikezawa and K. Aoyagi: J. Phys. Soc. Jpn. **58** (1989) 2276.

3)M. Fujita, H. Nakagawa, H. Matsumoto, T. Miyanaga, M. Watanabe, K. Fukui, E. Ishiguro, Y. Fujii and Y. Sakisaka: J. Phys. Soc. Jpn. **59** (1990) 338.

4)G. Hhapuis: Phys. Status Solidi a **43** (1977) 285.

5)H. Yamashita: J. Phys. Soc. Jpn. **29** (1990) 338.

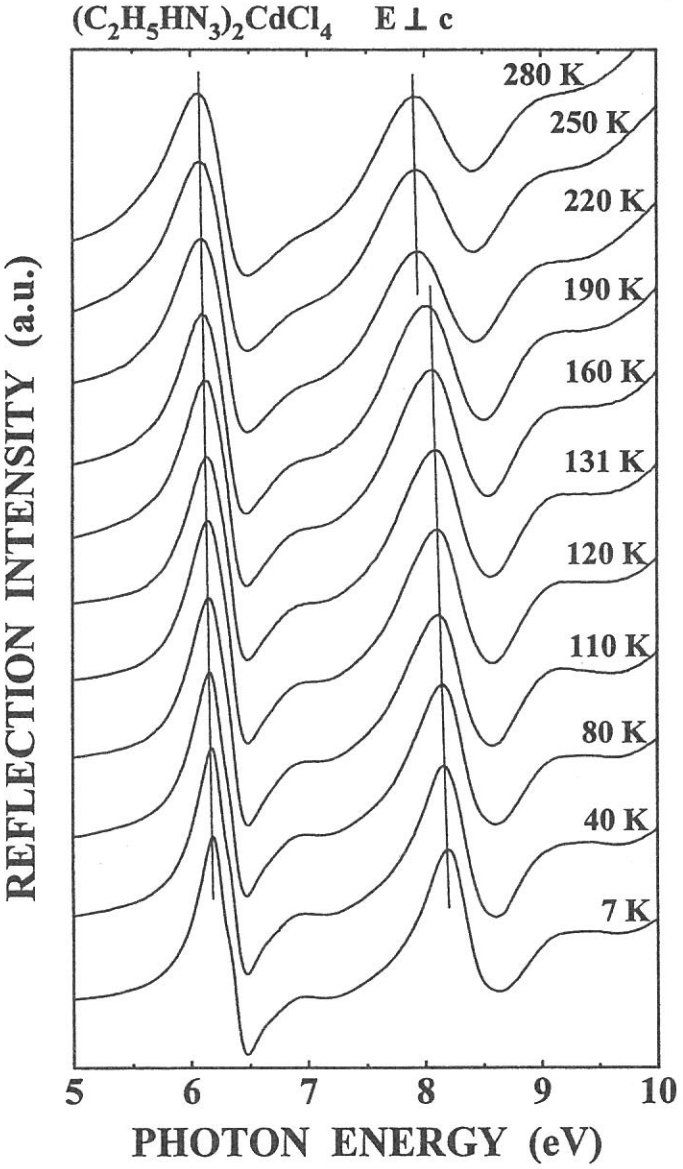

Figure 2

(BL1B)

Absorption Spectra and Optical Constants of Uniaxially Drawn Polyethylene Naphthalate Films

Isuke **OUCHI**, Ikuo **NAKAI**[A], Masao **KAMADA**[B] and Shin-ichiro **TANAKA**[B]

Faculty of Engineering, Tokushima Bunri University, Shido, Kagawa 769-2193
[A] Faculty of Engineering, Tottori University, Koyama, Tottori 680-8552
[B] UVSOR, Institute for Molecular Science, Myodaiji, Okazaki 444-8585

Polyethylene naphthalate (PEN) has a similar molecular structure as polyethylene terephthalate (PET), having a naphthalene ring in place of benzene in the main chain. As a film, it has somewhat better physical and chemical properties than PET in a practical sense; it is utilized for various products as electric insulators, capacitors, videotape bases, APS photographic bases etc. Structures and properties of PEN films have been studied by many researchers, but not so extensively as in PET. As for the electronic spectra, absorption spectra in solution[1] and in films[2] were reported; photochemical phenomena like coloration[3], fluorescence[4] have been treated to some extent; soft x-ray absorption was also studied[5,6]. However, the spectra relating to the deeper levels of valence electrons have not been examined so far; only a few studies have been made for PET too in this region.[7] The present study is being made to examine the electronic spectra of PEN in the deeper levels of valence electrons.

The measurement was made at the BL-1B where the Seya-Namioka type monochromator was equipped. Film samples of PEN were supplied from the Film Research Laboratory of Teijin Limited: amorphous undrawn films of 100 μm, uniaxially 4 times drawn films of 90 μm and biaxially drawn films of 40 μm.

The measurement procedure was the same as for the previous case of PET[8] but with an improvement. Namely, in the process of obtaining a reflection spectrum from a measured multiple reflection, more rigorous treatment was made for the spectrum in the semi-transparent region. Instead of approximating the calculated reflection to a straight line in the region, measured transmission data at each wavelength was put in the Kato's formula[9]; the transmission measurement was made separately by use of a Shimazu UV spectrometer: UV2400(PC)S.

Reflection spectra of PEN films uniaxially drawn by 4 times are shown in Fig.1 after correcting multiple reflection, where the reflection intensity of the film having its draw axis parallel to the electric vector of the incident light is more intense than that perpendicular, except in the region between 1600A and 2000A..

The phase of the reflected light was calculated from these data of reflection spectra using the Kramers-Kronig relation. Contribution to the integral from shorter and longer side wavelengths was counted by Roessler's method as in the previous study. Complex refractive indices and complex dielectric constants were computed by use of Fresnel equations; then, absorption coefficients were obtained from the extinction coefficients. Calculated refractive indices at 5000A agreed reasonably well with the values separately measured by Abbe's refractometer, guaranteeing the validity of the present treatment

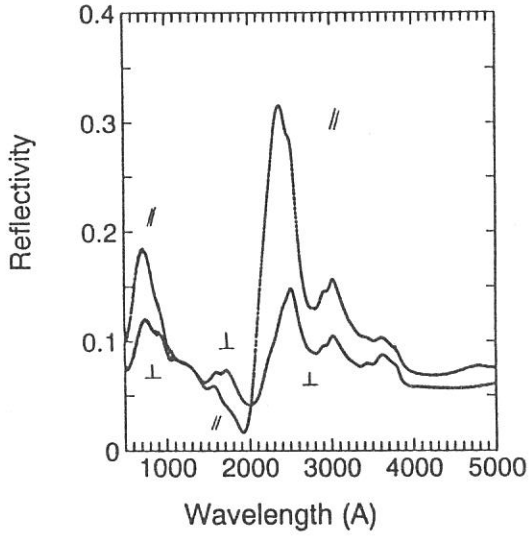

Fig. 1. Reflection spectra of uniaxially drawn (x4) PEN films. Multiple reflection is already corrected..

Fig. 2 shows the converted anisotropic absorption spectra of uniaxialy 4 times drawn PEN films. The absorption band of the longest wavelength has two peaks at 3560A and 3370A. They look rather perpendicular band; but it was slightly parallel according to the old data obtained by transmission method using extremely thin cast and drawn film. (Here, parallel band means that the electric vector parallel to the axial direction of the drawn film is absorbed more than that perpendicular to the axis, and perpendicular band is opposite.). Probably, the difference would be within the error caused by various approximation utilized in the Kramers-Kronig conversion. Nevertheless, the absorption coefficient at this band is much larger than that of the longest wavelength in a uniaxially drawn PET film. Second band is of parallel polarity and has three peaks at 2990A, 2890A and 2760A. Third band is very intense and has also parallel polarity and peaks at 2500A, 2390A and 2250A. Fourth band is perpendicular and peaks at 1700A. Polarity of the band peaking at 1550A is difficult to tell. Sixth band at 800-900A is strong and also has about same intensity either for parallel and perpendicular. General feature of the absorption spectra looks similar to that of PET exhibited in the previous report[8], whereas the detail is fairly different.

As an example of the optical constants obtained, refractive index and extinction coefficient of the uniaxially drawn (x4) PEN of parallel alignment is shown in Fig. 3. Detailed analysis should still to be made.

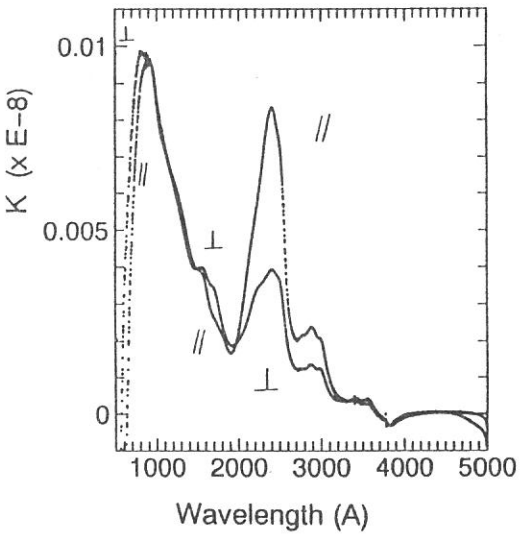

Fig.2. Converted absorption spectra of uniaxially drawn (x4) PEN films.

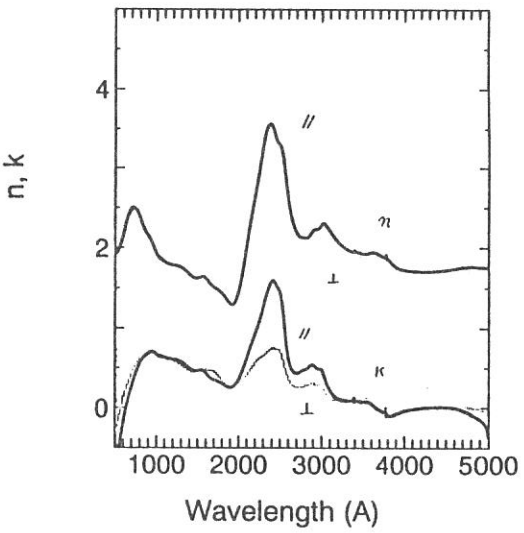

Fig. 3. Refractive index and extinction coefficient of a uniaxially drawn (x4) PEN films.

The authors are thankful to Mr. N. Takagi, Film Research Laboratory, Teijin Limited, for supplying film samples to us.

1) P-S.R. Chung et al., J. Appl. Polym. Sci., 24 (1979) 1809.
2) I. Ouchi, Rep. Progr. Polym. Phys. Jpn., 22 (1977) 437.
3) I. Ouchi et al., J. Appl. Polym. Sci., 20 (1976) 1983.
4) I. Ouchi et al., Polym. Adv. Technol., 10 (1999) 195.
5) I. Ouchi et al., Polym., J., 27 (1995) 127. J. Electr. Spectr. Rel. Phenom., 78 (1996) 363.
6) E.G. Rightor et al., J. Phys. Chem., 101 (1997) 1960.
7) M. Chitaib et al., Phys., Rev. B, 44(1997) 1960.
8) I. Ouchi et al., UVSOR Act. Rept. 1998, (1999) 88.
9) R. Kato, J. Phys. Soc. Jpn., 16 (1961) 2525.

(BL1B)

Reflection Spectra of Excitons in Orthorhombic $SnBr_2$

Yoshihiko YAMASAKI and Nobuhito OHNO

Division of Electronics and Applied Physics, Graduate School of Engineering, Osaka Electro-Communication University, Neyagawa 572-8530, Japan

Optical properties of Pb halides have been studied extensively so far by several groups. Especially, luminescence studies of these materials have been carried out since they give complimentary information on the photolysis phenomena. There are two types of luminescence in $PbCl_2$ and $PbBr_2$ at low temperatures [1,2]. One is the UV (B) luminescence produced under the excitation in the first exciton region, attributed to the radiative decay of self-trapped excitons at Pb^{2+} ion sites in $PbCl_2$ ($PbBr_2$). The other is the BG luminescence stimulated by photons with energies above the band gap, which originates from tunneling recombination of holes released from some trapping centers with electrons trapped at the Pb_2^{3+} self-trapped electron (STEL) centers [3].

Orthorhombic Sn halides, $SnBr_2$ and $SnCl_2$, have the same crystal structure (space group *Pmnb*) and the similar electronic configurations as orthorhombic Pb halides. It is interesting to know the electronic structures and exciton states in Sn halides. However, optical properties of these materials have not been revealed clearly so far [5-7]. In the present study , we have measured polarized reflection and absorption spectra of orthorhombic $SnBr_2$ using synchrotron radiation at the BL1B line of UVSOR facility.

Figure1 shows the reflection spectra up to 12 eV for polarization *E//a*, *E//b* and *E//c* measured at 12 K. As clearly seen, structures in the energy region of 3-8 eV show pronounced polarization dependence. The reflection spectra at the absorption edge are shown in expanded scale in Fig. 2. We can see a prominent peak at 3.409 eV for *E//a*, two peaks at 3.410 eV and 3.463 eV for *E//b*, and a peak at 3.461 eV and a weak hump at 3.412 eV for *E//c* polarization. These structures are obviously ascribed to the lowest exciton transitions. The splitting energy of the exciton for *E//b* polarization is 53 meV. The observed first exciton peaks in $SnBr_2$ are considerably sharp as compared with those in orthorhombic Pb halides. The polarization dependence of the first exciton band is well interpreted as a cationic interband transition in Sn^{2+} ($5s \rightarrow 5p$) under the crystal field with C_S symmetry.

We can see a small hump on the higher energy side of the first exciton band for *E//b* and *E//c* polarizations as indicated by arrows in Fig. 2. They are located at 3.486 eV for *E//b* 3.485 eV for *E//c*, probably due to n=2 state of exciton Rydberg series. The exciton binding energy is estimated as 32 meV assuming the hydrogen-like energy model. It is to be noted that there has been no report on the observation of higher exciton series in orthorhombic Pb halides.

Absorption spectra near the fundamental absorption edge were also measured in the temperature range 10 to 300 K. The logarithmic plot of the absorption spectrum near the absorption edge is found to give a straight line, that is, the absorption tail of $SnBr_2$ is well described as Urbach rule. Temperature dependence of the Urbach slope gives the high-temperature value of the steepness parameter $\sigma_0 = 0.74$ (0.70) and the

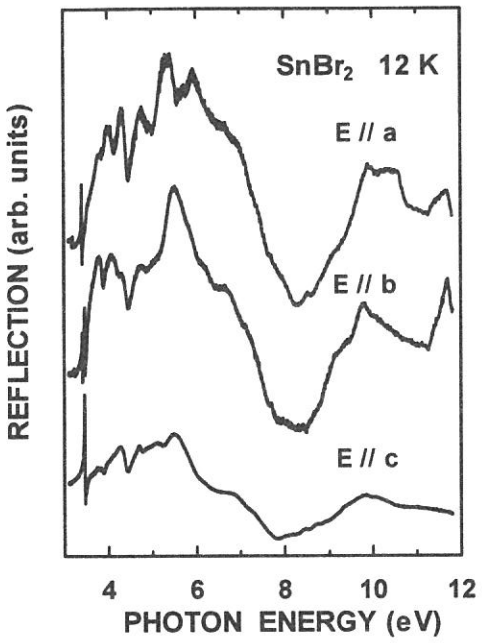

Fig. 1. Polarized reflection spectra of orthorhombic $SnBr_2$ at 12 K.

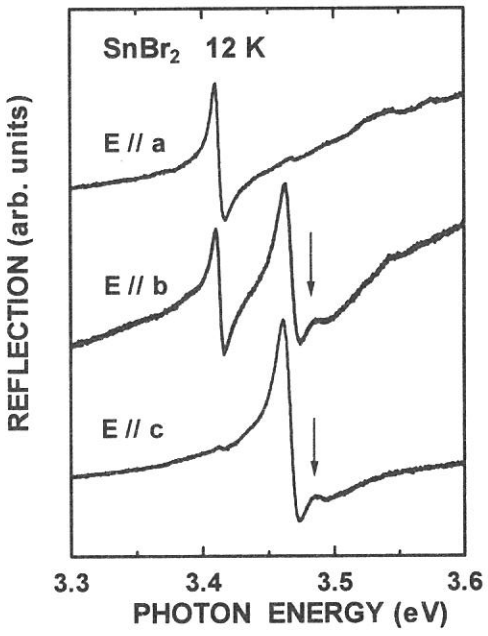

Fig. 2. Polarized reflection spectra of $SnBr_2$ in the first exciton region measured at 12 K.

effective phonon energy $h\omega_p = 24$ meV (13 meV) for $E//a$ ($E//b$) polarization. The small values of σ_0 indicate that the exciton-phonon interaction is in a strong case, and the excitons are unstable and easily self-trapped in $SnBr_2$.

In summary, polarized reflection spectra of orthorhombic $SnBr_2$ have been investigated by using synchrotron radiation. The first exciton bands with pronounced polarization dependence have been found at around 3.4 eV in the reflection spectra. Absorption spectra near the fundamental absorption edge are found to obey Urbach rule, suggesting that excitons are self-trapped in $SnBr_2$.

References

[1] M. Kitaura and H. Nakagawa: J. Electron Spectrosc. and Relat. Phenom. **9** (1996) 171.
[2] M. Kitaura and H. Nakagawa: J. Lumin. **72-74** (1997) 883.
[3] S.V. Nistor, E. Groovaert and D. Schoemaker: Phys. Rev. **B48** (1993)9575.
[4] M. Fujita, H. Nakagawa, K. Fukui, H. Matsumoto,T. Miyanaga and M. Watanabe: J. Phys. Soc. Jpn. **60** (1991) 4393.
[5] A.S. Voloshinovskii, S.V. Myagkota, N.S. Pidsyrailo and Z.A. Khapko: Opt. Spectrosc. (USSR) **52** (1982) 457.
[6] N.S. Pidsyrailo, A.S. Voloshinovskii, N.G. Stan'ko and Z.A. Khapko: Sov. Phys. Solid State **24** (1982) 708.
[7] A.S. Voloshinovskii: Phys. Solid State **35** (1993) 1588.

(BL1B)

Study on the defects in silica irradiated by a nuclear reactor

Tomoko Yoshida[1], Tetsuo Tanabe[1], Tatsuya Ii[2], Takanobu Hara[2], Shunsuke Muto[1] and Yoshitaka Inaki[3]

[1]*Center for Integrated Research in Science and Engineering, Nagoya University, Nagoya 464-8603, Japan*

[2]*Department of Nuclear Engineering, Graduate School of Engineering, Nagoya University, Nagoya 464-8603, Japan*

[3]*Department of Applied Chemistry, Graduate School of Engineering, Nagoya University, Nagoya 464-8603, Japan*

Introduction

Neutron irradiation and radiation effects on silica glasses are one of the main concerns for their application as optical windows, insulators and optical fibers in fusion reactors as well as fission reactors.[1,2] Recently, dynamic effects of the irradiation in silica glasses have been observed as degradations of their good transparency, high electrical resistivity, low optical absorption and luminescence during in-reactor irradiation.[1-5] In order to investigate dynamic effects of in-reactor irradiation on silica, we have tried to make in situ luminescence measurement of silica glasses induced by in-reactor irradiation. The in-reactor luminescence from silica was found to be a powerful technique to observe dynamic effects on the electrical property of silica, since the luminescence was directly associated with the electron excitation process under the irradiation. So far, we found that the luminescence mainly originates from the defects in silica due to an electron excitation during irradiation. However, the detailed dynamic effects on silica glass are still unknown. For example, the intrinsic defects existing in silica glasses make our understanding of the defects formation process very difficult. And the influence of the OH content in silica on the luminescence is also still an open question.

In the present study, optical absorption measurements for the irradiated samples have been carried out to obtain information of the defects produced by the reactor irradiation.

Experimental

The samples used in this work were fused silica glasses (T-1030 and T-2030) and synthesized silica glasses (T-4040) of 13 mm diameter and 2 mm thickness produced by Toshiba Ceramics, Japan with different OH content. Nominal impurity levels in these samples are listed in Table 1.

In-reactor irradiation have been carried out using the nuclear reactor YAYOI at the University of Tokyo. YAYOI was operated with a power of 0.5 or 1.5 kW (the neutron flux were about 2×10^{15} n/m^2 s and 6×10^{15} n/m^2 s, respectively) with an average neutron energy of 1.3 MeV and γ ray level was about 3.0 kGy/h.[6] The irradiation temperature was not controlled but kept below 323 K because of small output power of the reactor.

Optical absorption were measured at room temperature using synchrotron radiation at the beam line 1B station (BL-1B) attached with 1m Seya-Namioka monochromator at UVSOR, Institute for Molecular Science, Okazaki, Japan, operated at electron energy of 750 MeV. Optical absorption spectra were detected by a photomultiplier (Hamamatsu R105).

Results and Discussion

Fig. 1 shows the optical absorption spectra of low-OH fused silica glass (T-2030) irradiated in the reactor and that of unirradiated one. The fluence of the neutron in the irradiated sample was estimated as ca. 2.8×10^{19} n/m^2. In the spectrum of the unirradiated one (Fig. 1a), optical-absorption bands at ca. 5.1, 6.2 and 7.6 eV were observed, which is a clear indication of the existence of various intrinsic oxygen deficiencies in the unirradiated sample. The band at 7.6 eV is characteristic of the oxygen-deficient-type amorphous SiO_2 [7] and known as E center (≡Si-Si≡). And the absorption band appearing around 5 eV has been reported as the B_2 center [8] which has been attributed to either an oxygen vacancy (≡Si-Si≡) or twofold coordinated silicon (0-Si-0). The origin of the absorption band at around 6.2 eV is not clear, although this band was observed

for the KrF laser irradiated silica sample. [9] In the absorption spectrum of the irradiated sample (Fig. 1b), the band at 7.6 eV grow and a new band at 5.8 eV corresponding to E' center (≡Si) [10] appeared, indicating the increase in the number of E and E' centers by the in-reactor irradiation. On the other hand, as shown in Fig. 2a, the optical absorption spectrum of the unirradiated high-OH synthesized silica glass (T-4040) had no significant band in the region from 2 eV to 7.5 eV. The in-reactor irradiation (the neutron fluence of 2.7×10^{20} n/m^2) brought the intense absorption bands at 5.1, 5.8 and 7.6 eV assigned to B_2, E' and E centers. Thus, the optical absorption spectra clearly showed the production of various types of oxygen deficiencies such as B_2, E and E' by the irradiation. These defects should be produced mainly by the atomic displacement and electron excitation effects during in-reactor irradiation.

Table 1
Nominal impurity levels in silica glasses (in ppm)

Sample	Al	Fe	Na	K	Cu	B	OH
Fused silica (T-1030)	8	0.4	0.8	0.8	0.02	0.3	200
Fused silica (T-2030)	8	0.8	1	1	0.02	0.3	1
Synthesized silica (T-4040)	0.1	0.05	0.05	0.05	<0.01	<0.01	800

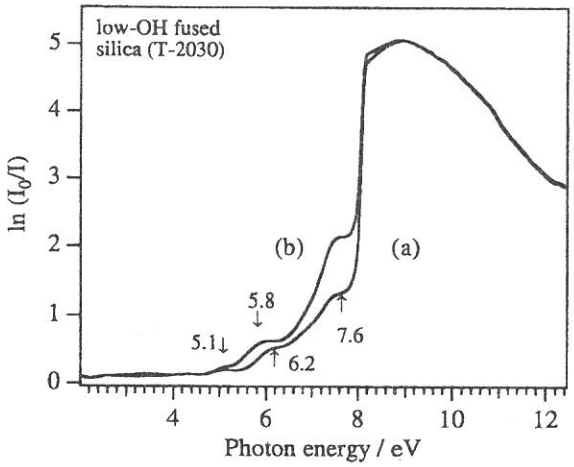

Fig. 1 Optical absorption spectra of (a) an unirradiated low-OH fused silica glass (T-2030) and (b) the reactor irradiated one (neutron fluence is 2.8×10^{19} n/m.)

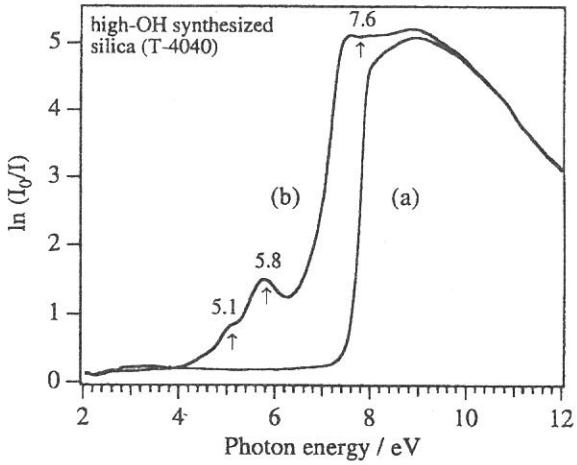

Fig. 2 Optical absorption spectra of (a) an unirradiated high-OH synthesized silica glass (T-4040) and (b) the reactor irradiated one (neutron fluence is 2.7×10^{20} n/m.)

References

[1] F. W. Clinard, Jr and L.W. Hobbs, Physics of Radiation Effects in Crystal (Elsevier, Amsterdam, 1986) p. 442.

[2] Proc. US/Japan Workshop on Dynamic Effects of Irradiation in Ceramics, Santa Fe, November 11-14,1992, Los Alamos National Laboratory Report LA-UR-92-4400 (1992)

[3] E. H. Farnum et al., J. Nucl. Mater. 191/194 (1992) 548.

[4] E. R. Hodgson, J. Nucl. Mater. 191/194 (1992) 552.

[5] T. Shikama et al., J. Nucl. Mater. 191/194 (1992) 544 and 575.

[6] M. Nakazawa and A. Sekiguchi, Radiation Dosimetry Data for Reactor YAYOI, Interior Report of University of Tokyo, R0037 in Japanese.

[7] R. Tohmon, H. Mizuno, Y. Ohki, K. Sasagane, K. Nagasawa and Y. Hama, Phys. Rev. B 44 (1989) 1337.

[8] L. Skuja, J. Non-Cryst. Solids 149 (1992) 77.

[9] A. Anedda, C. M. Carbonaro, R. Corpino and F. Raga, Nucl. Instr. and Meth. B 141 (1998) 719.

[10] R. Boscaino, M. Cannas, F. M. Gelardi, M. Leone, Nucl. Instr. and Meth. B 116 (1996) 373.

(BL3A1)

Amplification of impurity-associated Auger-free luminescence in $Rb_{1-x}Cs_xCl$ (x = 0.18) mixed crystals by undulator radiation

M. Itoh, S. Asaka,[1] M. Kamada[2] and V. B. Mikhailik[3]

Faculty of Engineering, Shinshu University, Nagano 380-8553

[1] *Equipment Development Center, Institute for Molecular Science, Okazaki 444-8585*

[2] *UVSOR Facility, Institute for Molecular Science, Okazaki 444-8585*

[3] *Lviv Franko State University, Kyryla i Mefodia str.8, 290005, Lviv, Ukraine*

A new mechanism of light amplification and laser action effects has been examined in BaF_2 [1], for which the hole transitions between the core and valence bands have a primary importance. This experiment has demonstrated a principal possibility to achieve lasing in compounds exhibiting Auger-free luminescence (AFL). Since the AFL arises from radiative transitions between the completely filled valence and core bands, the creation of empty (hole) states in the lower core bands means formation of the inverted population between these two bands at any excitation intensity. This idea was successfully tested in BaF_2 [1], but, as it turned out, the certain threshold of pumping power was needed to the amplification. This is probably because a part of the AFL is reabsorbed by metastable self-trapped exciton states in BaF_2. It is of great interest to extend similar experiments to other AFL-emitting materials in order to test their potentialities for laser action.

The compounds exhibiting impurity-associated AFL are supposed to be very promising candidates for the purpose mentioned above. This type of luminescence has been found in AFL-free alkali halides containing alkali or halogen impurity ions that form the impurity states in the energy gap between the host valence and outermost-core bands, which provides an additional channel for radiative decay of the core holes generated on the impurity states. The impurity-associated AFL yield in $Rb_{1-x}Cs_xCl$ can exceed the intrinsic AFL yield in pure CsCl [2]. In the present experiment, we have thus investigated this mixed crystal with x = 0.18.

The undulator radiation at BL3A1 provides quasi-monochromatic light with $\Delta\lambda/\lambda$ = 5% at 36 eV (photon flux: ~ 10^{15} photons/sec·mm^2) and at 15 eV (photon flux: ~ 10^{14} photons/sec·mm^2). A freshly cleaved 1 mm-thick sample was mounted on a rotatable holder installed in a vacuum chamber. The undulator radiation was incident at nearly 45° on the sample surface. Two flat multiple-dielectric coated mirrors (the reflectivity R = 100 and 90% in the 260-320 nm range) were placed near the sample in the direction perpendicular to the exciting radiation. The best collimation of the optical cavity was attained when the images of the iris diaphragms formed by He-Ne laser light reflected from the front and back mirrors were coinciding with each other. The luminescence was observed without using lenses through a monochromator equipped with a PM tube. A single-photon counting technique was applied to decay profile measurements. All the experiments were performed at room temperature.

Figure 1 shows luminescence spectra taken under no collimation (broken line) and the best collimation (solid line). The excitation was made with 36-eV photons, which corresponds to the transition from the deep-lying Rb 4p core state to the conduction band. The AFL spectra consist of the main band at 275 nm, the high-

energy band at 240 nm and the low-energy tail around 325 nm. An important feature in Fig. 1 is that the peak intensity of the 275-nm band is enhanced by a factor of 2.6 when the mirrors are adjusted for the best collimation. Similar enhancement was also confirmed under the excitation with 15-eV photons, corresponding to the Cs 5*p* core state → conduction band transition. The enhancement factor was about 1.7 in this case, in spite of the fact that the photon flux at 15 eV is one order of magnitude smaller than that at 36 eV. Furthermore, from Fig. 1, one may see a sharpening of the 275-nm band under the best collimation. These observations indicate the amplification of the impurity-associated AFL in $Rb_{1-x}Cs_xCl$ mixed crystals.

In the lower part of Fig. 2 are shown decay profiles of the 275-nm band excited with 36-eV photons under (a) the best collimation and (b) no collimation. By assuming a single exponential decay for the curve (b), we obtained a decay constant of 0.9 ± 0.1 nsec, in good agreement with the previous result. The decay profile of curve (a) is different from that of curve (b). This fact is clearly seen in the upper part of Fig. 2, where the dotted curve was obtained by subtracting the curve (b) from the curve (a). It appears that a faster component grows up in the peak region of the curve (a). Such a shortening of the luminescence decay profile is a characteristic feature of stimulated emission.

The above results confirm the validity of our anticipation about the promising potentialities of the compounds with impurity-associated AFL for light amplification, using the inverted population arising from impurity-core level excitation.

The authors acknowledge Mr. Y. Bokumoto and Mr. J. Murakami for their assistance in the experiment.

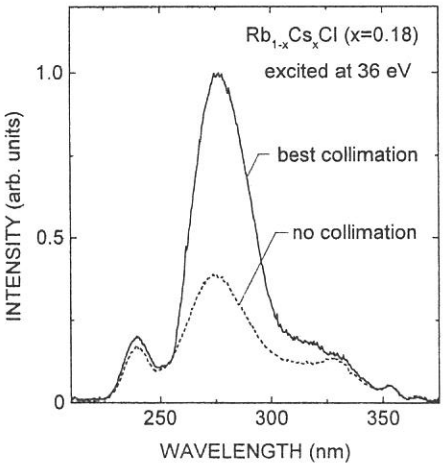

Fig. 1. Luminescence spectra of $Rb_{1-x}Cs_xCl$ (x = 0.18) excited with 36-eV photons under no collimation and the best collimation.

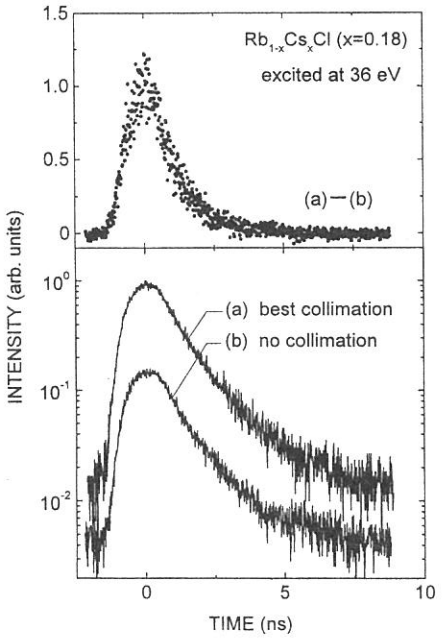

Fig. 2. Decay profiles of the 275-nm band excited at 36 eV; lower part. Subtraction of (b) from (a); upper part.

[1] M. Itoh and H. Itoh: Phys. Rev. B **46** (1992) 15509.

[2] A. S. Voloshinovskii, M. S. Mikhailik, V. B. Mikhailik, E. N. Mel'chakov, P. A. Rodnyi, C. W. E. van Eijk and G. Zimmerer: J. Lumin. **79** (1998) 107.

(BL5B)

Optical Properties of Amorphous Chalcogenide Semiconductors

Koji HAYASHI

Department of Electrical and Electronic Engineering, Gifu University, Gifu 501-1193, JAPAN

Amorphous chalcogenide semiconductor materials, such as a-As_2S_3, a-As_2Se_3 and a-Se etc., show a variety of photoinduced phenomena. Therefore, these materials are expected as materials for optoelectronic devices. A lot of work have been done on the photoinduced phenomena of these amorphous semiconductor materials and various mechanisms have been proposed for these photoinduced phenomena[1,2]. However, the details of the mechanisms are still unknown. These phenomena were studied by exciting outer core electrons with the irradiation of the visible light with the energy corresponding to the optical bandgap or sub-bandgap. Little attention has been give to photoinduced effects by exciting inner core electrons with the irradiation of higher energy photon. To obtain a wide knowledge of the photoinduced effects, it is necessary to investigate photoinduced phenomena on wide energy region. In the previous reports[3,4], we reported the photoinduced effects in amorphous chalcogenide films by the irradiation of the vacuum ultra-violet (VUV) light. That is, photodarkening is occurred by the irradiation of the VUV light and the darkened state is removed by annealing at near the glass-transition temperature. In our recent study, we observed interesting photoinduced change in the photoconductivity and the total photoyield of amorphous chalcogenide films by the irradiation of the VUV light[5-7]. In the present work, we measure the VUV reflection spectra and the total photoyield spectra in these materials in order to study the photoinduced effects of those optical spectra by the irradiation of the bandgap light and the VUV light.

The samples used for measurements were amorphous arsenic trisulfied (a-As_2S_3). Thin films of a-As_2S_3 were prepared onto quartz substrates by conventional evaporation technique. For the measurements of the total photoyield spectra, an electrode using Al contact was fabricated first on the substrate before depositing the amorphous film. A typical thickness of an amorphous film was around 0.7 μm. The samples were annealed at 443K (near the glass transition temperature) for two hours in a vacuum. The experiments were performed at room temperature at the BL5B beam line of the UVSOR facility of the Institute for Molecular Science in Okazaki. For the measurements of the reflection spectra, the incident angle was near normal to the sample surface and the reflectivity was measured by a silicon photodiode. The reflection spectra were obtained by normalizing the spectra by the spectrometer system response.

Figure 1 shows the VUV reflection spectrum of a-As_2S_3 at room temperature in the photon energy region between 35 eV and 55 eV. One main peak and interfering pattern were observed at this energy region. This peak around 44 eV corresponds to the 3d core level of As atom. Figure 2 shows the total photoyield spectrum of a-As_2S_3 at room temperature in the same photon energy region. As you see in the figure, the peak corresponding to the 3d core level of As atom was also observed in the total photoyield spectrum. Further analysis of these spectra is now in progress. We pay attention to the photoinduced effects near this energy region. We now are investigating photoinduced change on these spectra. The detailed experiments and analysis will be done in the next step.

This work was partly supported by grants-in-aid for Scientific Research from the Ministry of Education, Science and Culture of Japan and the OGAWA Science and Technology Foundation

REFERENCES

[1] Ke. Tanaka, Rev. Solid State Sci., 4(1990)641.
[2] K. Shimakawa, A. Kolobov, and S. R. Elliott, Adv. Phys., 44(1995)475.
[3] K. Hayashi, D. Kato, and K. Shimakawa, UVSOR Activity Report 1995, p128.
[4] K. Hayashi, D. Kato, and K. Shimakawa, J. Non-Cryst. Solids., 198-200(1996)696.
[5] K. Hayashi, A. Hirai, and K. Shimakawa, UVSOR Activity Report 1996, p116.
[6] K. Hayashi, UVSOR Activity Report 1997, p118.
[7] K. Hayashi, UVSOR Activity Report 1998, p105.

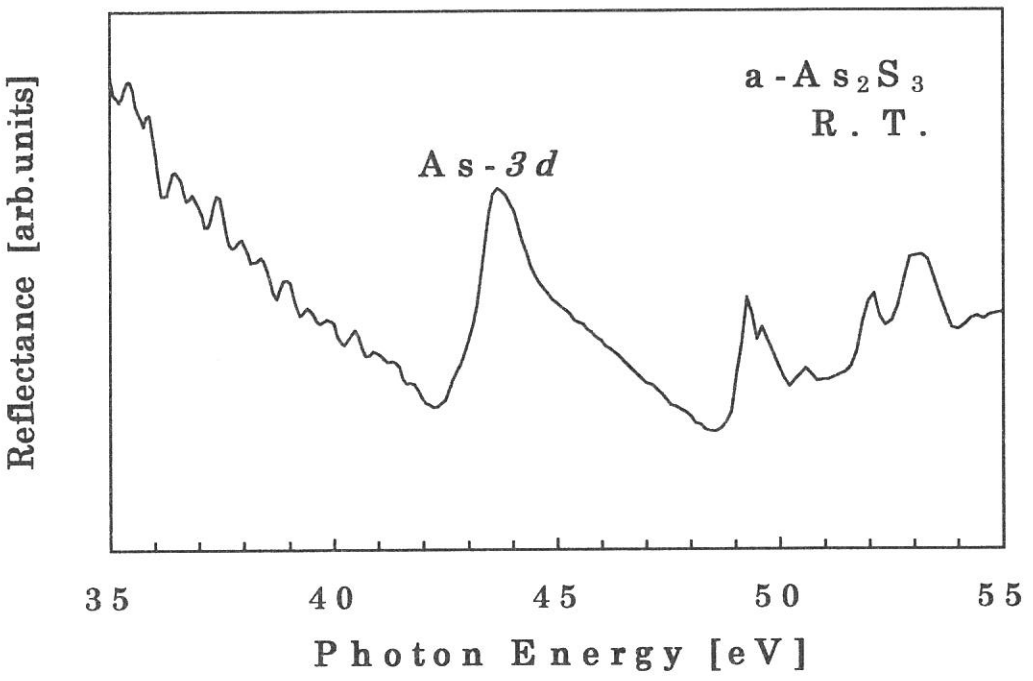

Fig. 1 Reflection spectrum of a-As_2S_3 at room temperature.

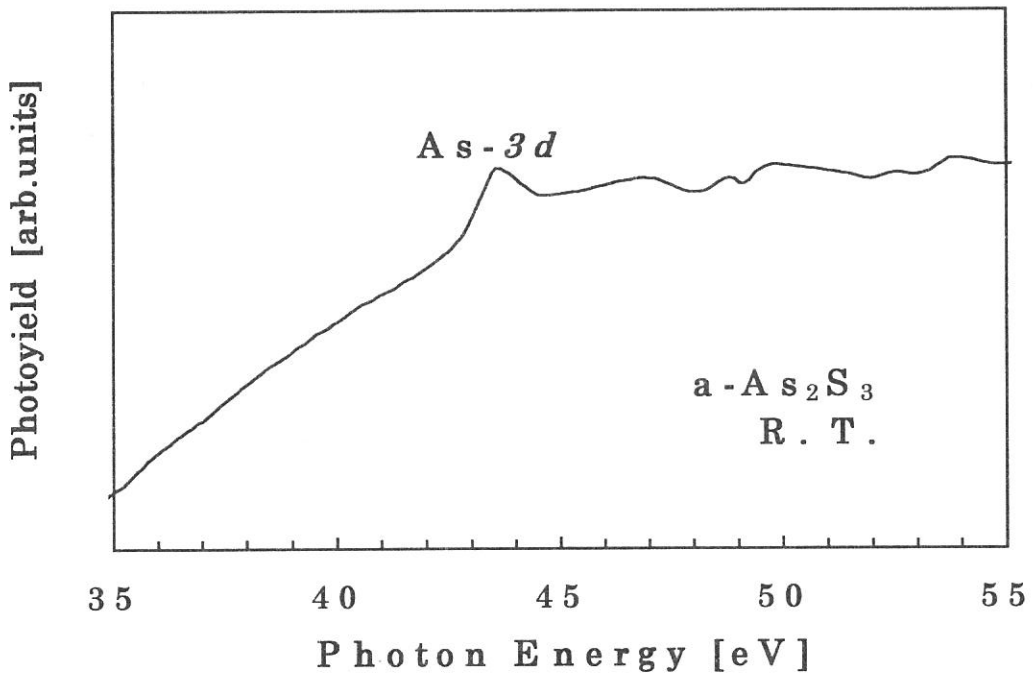

Fig. 2 Total photoyield spectrum of a-As_2S_3 at room temperature.

Vacuum-ultraviolet reflectance spectroscopy of transition-metal oxides

Yasujiro TAGUCHI[1], Eiji SAITOH[1], Yoshinori ONOSE[1],
Tadayuki OSAKI[1], Kyoko ISHIZAKA[1], Taka-hisa ARIMA[2], and Yoshinori TOKURA[1]

[1]*Department of Applied Physics, University of Tokyo, Tokyo 113-8656*
[2]*Institute of Materials Science, University of Tsukuba, Tsukuba 305-8573*

The discovery of high-Tc cuprate superconductor by Bednorz and Muller in 1986 has aroused great interest in strongly correlated electron systems in general, and 3*d* transition-metal oxides in particular. One of the most important characteristics for the correlated electron systems is the drastic re-construction of electronic structure over an energy scale of eV with changes of temperature, doping concentration, and/or external field. Therefore, optical reflectivity measurement over a wide energy range and the optical conductivity spectra derived from the reflectivity spectra provide us with very useful information about the strongly correlated electron systems.

In this beam time, we measured the reflectivity spectra of several transition-metal oxides, including Mn-, Ni-, Cu-, and Mo-oxides, for an energy range of 4 eV < E < 35 eV at room temperature. The measured reflectivity data, together with the lower-enegy data measured at University of Tokyo, were used to derive the optical conductivity spectra or dielectric function via the Kramers-Kronig analysis. As an example, the imaginary part of the dielectric function of pyrochlore-type Mo-oxide is shown below. This compound is known as showing geometrical frustration of magnetism, and exhibits an anomalous ferromagnetic state at low temperatures. The absorption bands indicated as A and B correspond to transitions from O 2*p* to Mo t_{2g} state and the bands denoted as C and D are due to the transition between O 2*p* and Mo e_g levels. The splitting (A and B, C and D) may be caused by the final state Hund's-rule coupling with the Mo t_{2g} spin. The structure indicated as E and the broad band lying at its higher-energy side correspond to the transition from O 2p to Sm 5d and/or Mo 5s/5p states.

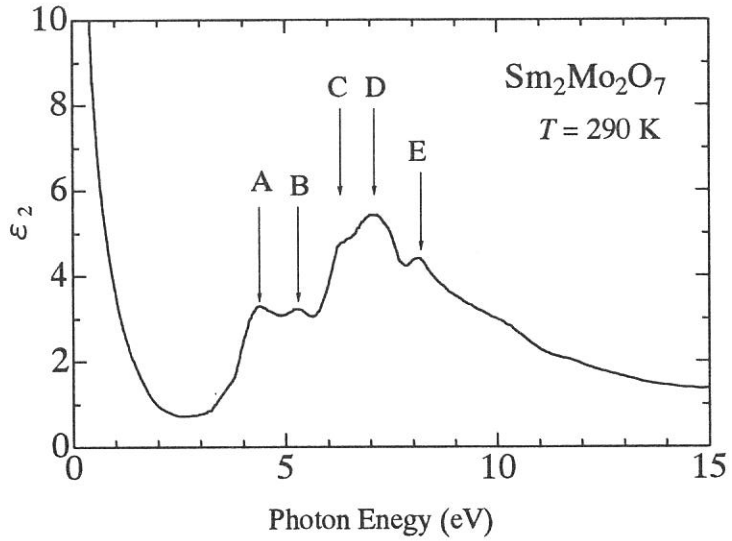

(BL6A1)

Temperature Dependence Millimeter Wave Reflection Measurements of Secondary Battery Substances $Li_{1-x}Ni_{1+x}O_2$

Hitoshi Ohta, Atushi Ueda, Yuichi Miura, Kenji Hazuki, Takao Nanba[A], Atushi Hirano[B] and Ryoji Kanno[B]

Department of Physics, Faculty of Science, Kobe University, 1-1 Rokkodai, Nada, Kobe 657-8501
[A]The Graduate School of Science and Technology, Kobe University, 1-1 Rokkodai, Nada, Kobe 657-8501
[B]Department of Chemistry, Faculty of Science, Kobe University, 1-1 Rokkodai, Nada, Kobe 657-8501

Recently, the study of $LiNiO_2$ is interesting because it is a promising material for the positive electrode of the Li ion secondary batteries. We found the drastic increase of the reflection of $LiNiO_2$ above 300 K in the millimeter wave region previously [1, 2]. We suppose that this increase of reflection is related to the motion of Li ion in the system. We extended our study to the low energy region down to 5 cm^{-1} and also trying to extend to the study of $Li_{1-x}Ni_{1+x}O_2$ [3, 4]. This year we extended our study to x=0.11 case.

The reflection measurements of x=0.11 sample have been performed in the spectra region from 5 to 60 cm^{-1} using the beam line BL6A1 of UVSOR. For the measurement below 22 cm^{-1}, low pass filter was used. The temperature was changed from 79 to 380 K. The gold plate was used as a reference and InSb detector was used as a detector. Figure 1 shows our results for x=0.11 sample. Overall reflection is low compared to the previous results of x=0 and x=0.05 samples [4]. Especially the increase of the reflection of x=0.11 sample is small as the temperature is increased above 300 K. The reflection above 300 K statrts to increase from 50 cm^{-1} in the case of x=0.11 while that of x=0 sample increase steeply below 10 cm^{-1}. Comparing three samples, which are x=0, 0.05 and 0.11, the increase of the reflection becomes steeper as x is decreased. This tendency seems to have correlation with the fact that the non-stoichiometry degrades the charge and discharge characteristics significantly. From the point of view of the application, the reflection measurements of $Li_{1-x}NiO_2$ are important as a next step.

[1] H. Ohta *et al.*: UVSOR Activity Report 1996 (1997) 182.
[2] H. Ohta *et al.*: proceedings of ICTMC (2000).
[3] H. Ohta *et al.*: UVSOR Activity Report 1997 (1998) 128.
[4] H. Ohta *et al.*: UVSOR Activity Report 1998 (1999) 158.

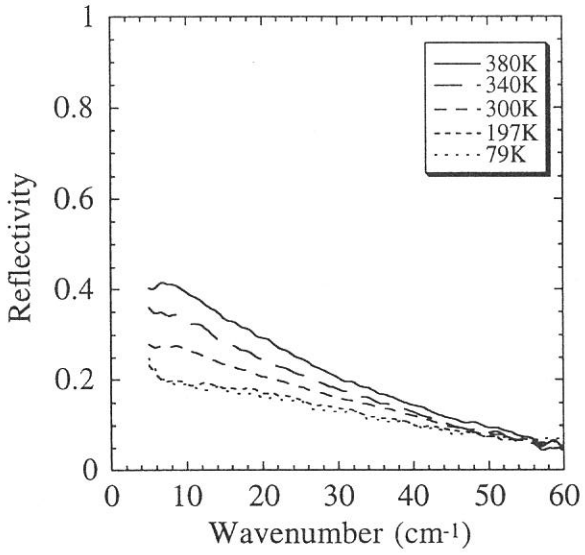

Fig. 1 The reflection spectra of x=0.11 sample.

(BL6A1)

Optical Response Of $CuIr_2X_4$ (X=S,Se) Due To Metal-Insulator Transition

M.Hayashi[1], M.Nakayama[1], T.Nanba[1], T.Matsumoto[2], J.Tang[2] and S.Nagata[3]

1.*Graduate School of Science and technology, Kobe University, Nada-ku, 657-8501, Kobe, Japan*

2.*National Research Institute for Metals, 1-2-1Sengen, Tsukuba, 305-0047, Japan*

3.*Department of Materials Science and Engineering, Muroran Institute of Technology, 27-1 Mizumoto-cho, Muroran, 050-8585, Japan*

$CuIr_2X_4$(X=S,Se) are spinel-type compound. $CuIr_2Se_4$ is a metal at atmospheric pressure but shows a stabilization of insulating phase from metal phase under high pressure [1]. $CuIr_2S_4$ undergoes a temperature-induced metal-insulator transition (M-I transition) at around 226K [2,3]. The magnitude of the energy gap in the insulating phase was estimated to be 0.094 eV by the electric resistivity data in the temperature range between 140K and 200K.[1,2] From X-ray diffraction measurement[3], $CuIr_2S_4$ was found to possess a normal cubic structure in the metallic phase and to be distored to a tetragonal structure in the insulating phase. However, additional some superstructure spots that cannot be assigned simply by tetrahedrally distored spinel structure were found in the low phase. The details of the structure is still unknown in the insulating phase.[3] Band calculations[4] based on a FLAPW method and photoemission data [5] showed the existence of Ir5*d*-S3*p* hybridization band near the Fermi level (E_F). It is therefore very interesting to know the fine electronic structure very close to the E_F by low energy optical excitation methods.

The temperature dependence of the optical reflection spectrum of the polycrystalline sample of $CuIr_2X_4$ (X=S and Se) was measured in the energy region of 0.005-6 eV. The energy resolution was kept to be 4 cm^{-1}. In the energy range below 0.015 eV, infrared synchrotron radiation at the UVSOR Facility of Institute for Molecular Science in Okazaki was used as a light source using a Martin-Puplett interferometer. The optical conductivity spectrum ($\sigma(\omega)$) was obtained from a Kramers-Kronig transformation of the R- spectrum. which was extrapolated by Hagen-Rubens' relation $R(\omega) \propto 1 - a\sqrt{\omega}$ in the lower energy side of the spectrum and by a well known function of $R(\omega) \propto b\omega^{-4}$ in the higher energy side.

Figs.1 and 2 show the measured R- (*a*) and the σ-spectra (*b*) of $CuIr_2S_4$ and $CuIr_2S_{e4}$ at various temperatures. From the Drude-like R spectra, $CuIr_2S_{e4}$ was found to hold metallic properties through the whole temperature range at atmospheric pressure although it exhibits the R-spectra with many peaks structure as cooling down to 30 K. On the other hand, the R-spectrum of $CuIr_2S_4$ showed a strong temperature-dependence. Above 222 K, the R-spectra showed an abrupt rise below 0.3eV which corresponds to a so-called plasma frequency due to the collective motion of free carriers. As temperature decreases below 221 K, such metallic behavior was completely suppressed (the occurrence of M-I transition) and many phonon-like structures appeared in the narrow energy region of 0.035eV-0.052eV. In the insulating phase, the energy gap was estimated to be about 0.1eV from the abrupt decrease in the intensity of the σ-spectra, which is almost consistent with 0.094eV given by electric resisitivity data [1,2]. A new band appeared at 0.4eV and gradually grew instead of the band around 0.7eV in the metallic phase as cooling, so as to compensate the decrease in intensity of the Drude component. In this way, by low energy optical excitation experiment, we resolved the fine change in the electronic structure within the overall change in the density of state observed in the photoemission spectroscopy. The σ-spectrum in the metallic phase was well fitted by the superposition of two Drude and two Lorentz functions (see Fig. 3). The existence of two Drude components suggests that at least two kinds of energy levels go across the E_F. This is consistent with the band calculation results of $CuIr_2S_4$ which indicates two conduction bands in the direction of X-Γ of the B.Z. Conduction bands in $CuIr_2S_4$ consist mainly of Ir5*d* and S3*p* hybridization.

References
[1]J.Tang,T.Furybayashi,T.Kosaka,s.Magata,Y.Kato,h.Asano,and T.Matsumoto, Rev.High Pressure Sci. Technol. 7(1998)496.
[2] S.Nagata, T.Hagino, Y.Seki and T.Bitoh, PhysicaB 194-196 (1994) 1077.
[3]T.Furubayashi, T.Matsumoto, T.Hagino, S.Nagata, J.Phys.Soc.Jpn 63 (1994) 3333.
[4]T.Oda, M.Shirai, N.Suzuki and K.Motizuki, J.Phys.:Condens.Matter 7 (1995) 4433
[5]J.Matsuno, T.Mizokawa, A.Fujimori, D.A.Zatsepin, V.R.Galakhov, E.Z.Kurmaev,Y.Kato and S.Nagata, Phys.Rev.B 55 (1997) 15979.

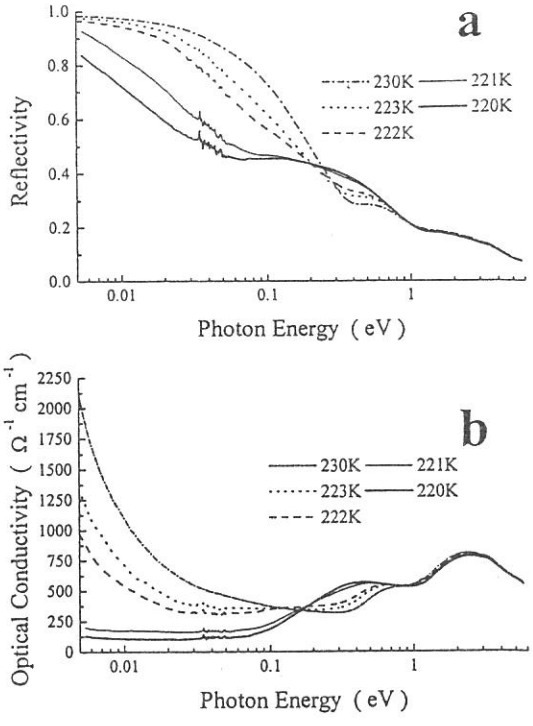

Fig.1 Reflection (*a*) and the σ-spectra (*b*) of $CuIr_2S_4$ at the temperatures of 230-220 K.

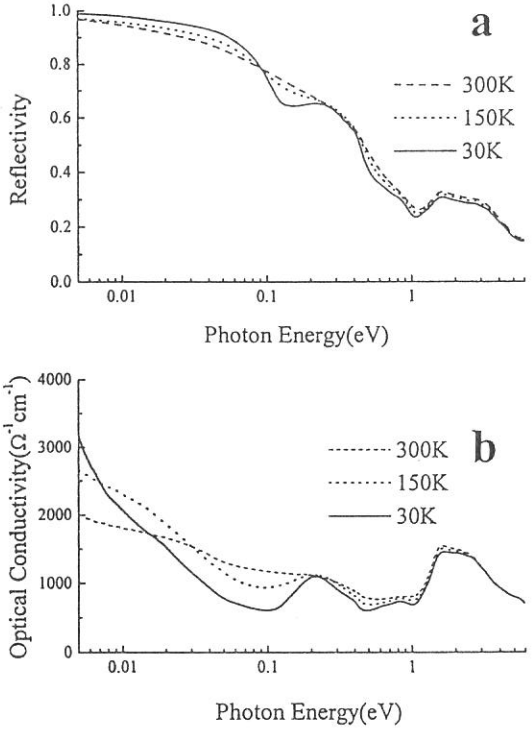

Fig.2 Reflection (*a*) and the σ-spectra (*b*) of $CuIr_2Se_4$ at 300,150 and 30K.

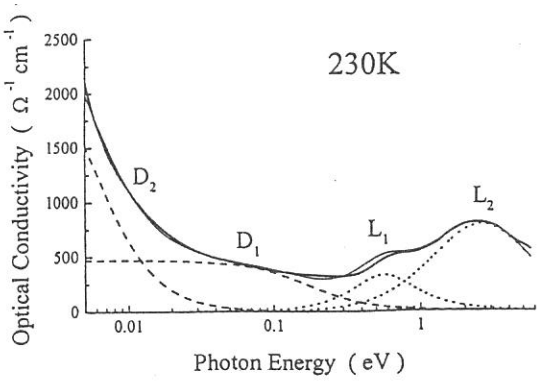

Fig3. Decomposition of the σ-spectrum of $CuIr_2S_4$ at 230K into two Drude (D_1 and D_2) and two Lorentz (L_1 and L_2) functions. The thick solid line represents an experimental curve and the thin solid one the summation of the fitting curves.

(BL6A1)

Optical Conductivity Spectra in the Magnetically Ordered States of CeBi

Shin-ichi Kimura[1], Mitsuru Okuno[1], Hideaki Kitazawa[2], Giyu Kido[2] and Takashi Suzuki[2]

[1]*Graduate School of Science and Technology, Kobe University, Nada-ku, Kobe 657-8501*
[2]*Physical Properties Division, National Research Institute for Metals, 1-2-1 Sengen, Tsukuba, 305-0047*

Cerium-monopnictides (Ce*X*; *X* = N, P, As, Sb, Bi) have complex magnetic phase diagram with the eleven layered magnetic structure. The origin of the magnetic phase diagram and the magnetic structure attract attention and many experimental and theoretical researchers have been investigating over two decades.

Last year, we started the magnetic reflectivity (MR) and the magnetic circular dichroism (MCD) experiments of CeSb in the infrared region using UVSOR for the investigation of the electronic structure in the magnetically ordered states.[1] In this year, we performed the measurement of the MR and MCD of CeBi, that also has a complex magnetic phase diagram, and we report the experimental result in this paper.

CeBi was grown by the Bridgman method with a tungsten furnace.[2] The measured surface is along (100)-plane and was prepared by a cleavage in a helium atmosphere. Since the material is easy to be oxidized, it was mounted to the sample holder of a cryostat in the helium atmosphere and was set to the center of the superconducting magnet in a short time.

The temperature dependence of optical conductivity spectra of CeBi at zero magnetic field and the assigned magnetic structure by neutron scattering[3] are shown in Fig. 1. The spectrum strongly changes with temperature. Particularly, the spectrum in the AF1-phase is strongly changes with changing temperature in spite that this material in the temperature range is assigned in the same phase by neutron

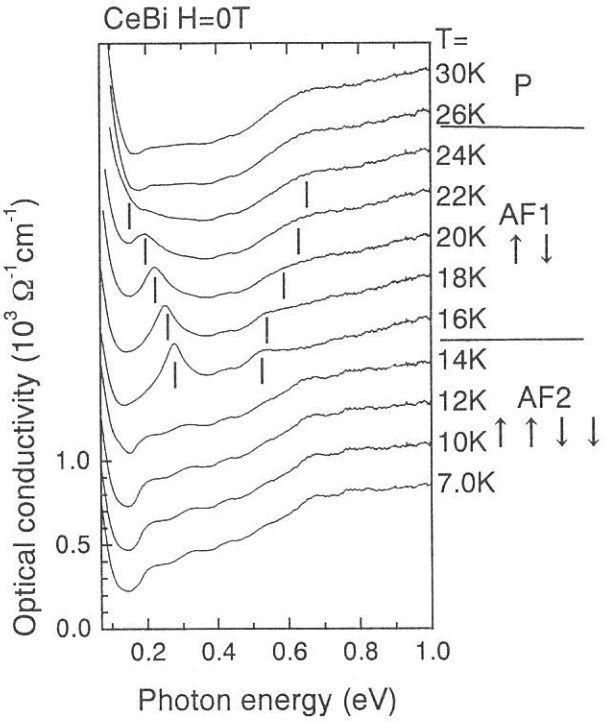

Fig. 1. Temperature dependence of the optical conductivity at zero magnetic field of CeBi. The depicted magnetic structures are referred from neutron scattering data.

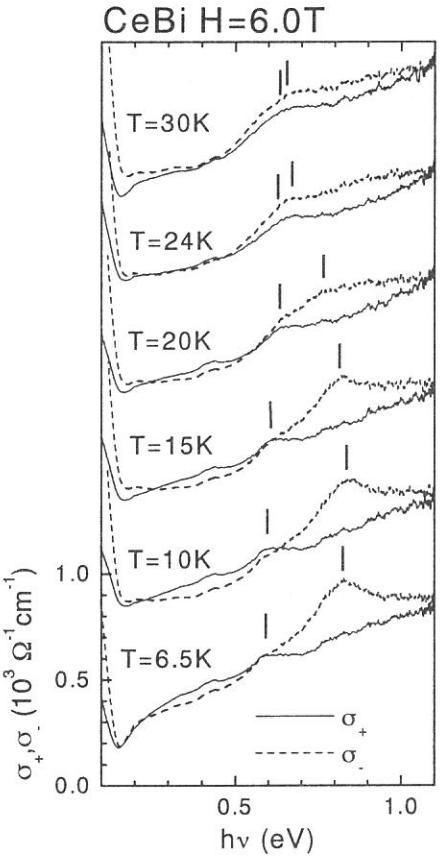

Fig. 2. Temperature dependence of the MCD optical conductivity ($\sigma_+(\omega),\sigma_-(\omega)$) at 6 T of CeBi.

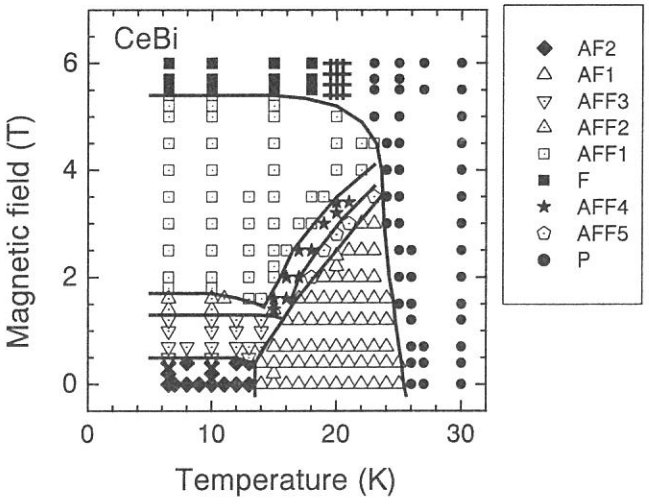

Fig. 3. Values of temperature and magnetic field at which magneto-reflectivity spectra of CeBi were measured. The same marks indicate the values at which same spectra are observed. The lines are where the spectrum changes. The legends have the same notation as those of neutron scattering.

scattering. One peak at 0.27 and one shoulder at 0.53 eV appear at 16 K and the energy separation of these structures increases as the temperature increases. At last, the spectrum continuously changes to that in the P-phase. The data indicate that the electronic structure in the AF1-phase strongly changes with the temperature and the electronic structure in the AF1-phase continuously connects to that in the P-phase.

The temperature dependence of the MCD optical conductivity spectrum at 6 T is shown in Fig. 2. Below 15 K, the $\sigma_+(\omega)$ and $\sigma_-(\omega)$ spectra are different from each other, *i.e.*, the peak of $\sigma_-(\omega)$ is located at 0.85 eV which is higher energy than that of $\sigma_+(\omega)$ at 0.6 eV. These spectra indicate that the electronic structure is the strong polarization. The state is assigned to be in the induced ferro-magnetic phase. However, these peaks approach each other around 20 K, and finally the $\sigma_+(\omega)$ and $\sigma_-(\omega)$ spectra become almost equal above 24K. Since the $\sigma_+(\omega)$ and $\sigma_-(\omega)$ spectra at 30 K are equal to the $\sigma(\omega)$ spectrum in the paramagnetic phase, the state at 6 T above 24 K is in the P-phase. Therefore the spectra indicate the state changes around 23 K from the induced ferro- to the para-magnetic phases. This is the first observation, because the phase transition has not been observed in neutron scattering experiment.[3]

According to the MR and MCD spectra, magnetic phase diagram was determined and is shown in Fig. 3. The outline of the diagram is almost equal to the previous one determined by neutron scattering.[3] Therefore the MR and MCD spectra reflect the electronic structure in the magnetically ordered states.

---

[1] S, Kimura *et al.*, J. Phys. Soc. Jpn. **69** (2000) in press.
[2] S. Kimura: Jpn. J. Appl. Phys. **38** (1999) Suppl. 38-1, 392.
[3] H. Bartholin *et al.*, J. de Phys. Colloq. **40** (1979) C5-130.

(BL6A1)

Optical response of RRu$_4$P$_{12}$ (R=La,Ce,Pr and Sm) due to metal-insulator transition

Masaya Nakayama[a] ,Masato Hayashi[a], Takao Nanba[a], Itimin Shirotani[b], and Chihiro Sekine[b]

a Graduate school of Science and Technology, Kobe University, Nada-ku, Kobe 657-8501, Kobe,Japan

b Muroran Institute of Technology, 27-1, Mizumoto,Muroran 050-0071, Japan

RRu$_4$P$_{12}$ (R=La,Ce,Pr and Sm) are ones of ternary metal phosphides with the skutterudite structure ($CoAs_3$-type) which is represented as RT_4P_{12} (R=rare earth element and T=transition metal). Recently, their stable compounds have been successfully synthesized using a wedge-type cubic anvil high pressure apparatus under a high pressure of 4 GPa and high temperature of 1100 ℃[1] According to the electric resistivity data, CeRu$_4$P$_{12}$ and CeFe$_4$P$_{12}$ are a semiconductor [1,2], LaRu$_4$P$_{12}$ shows a superconductivity at 7K, PrRu$_4$P$_{12}$ and SmRu$_4$P$_{12}$ show a metal-insulator (M-I) transition, respectively, at Tc=60K [3] and 16K.

After the success of the synthesis, many experiments has started on these compounds but the optical measurements has not yet been done.for these materials. We measured the reflection spectrum in order to know the electronic structure close to the Fermi energy level of these materials. The temperature dependence of the optical reflection spectra of RRu$_4$P$_{12}$ (R=La,Ce,Pr and Sm) were measured in the energy region of 0.005 -4 eV. The optical conductivity spectrum ($\sigma(\omega)$) was obtained from a Kramers-Kronig transformation of the reflectivity spectrum.

Figs.1 and 2 show the measured reflection and the optical conductivity spectra of these materials at 300 K (dashed line) , 78K (dotted line) and 8 K (solid line). We can see that the onset of the interband transition as the abrupt rise in the intensity of σ-spectra around 0.4 eV for La, Pr, and Sm compounds, and the spectral profile in the higher energy region than 0.4eV has a similar structure with three peaks. The similarity of the spectral profile means that the overall electronic structure of these three compounds (La,Ce,Pr and Sm) does not change. In CeRu$_4$P$_{12}$, the σ-spectrum did not show a temperature dependence. Then we can see that CeRu$_4$P$_{12}$ is semiconductor with an energy gap of about 0.2 eV. In addition, the spectrum profile in the higher energy region than 0.7eV has similar structure with those of other three compounds although the energy positions of three peaks shift to a higher energy side , and an additional peak exists at 0.4 eV. We found that the effective electron number which contributes to the Drude component of other three compounds is almost same with the effective electron number which contributes to the interband transition at 0.4 eV of CeRu$_4$P$_{12}$. In the insulating phase of PrRu$_4$P$_{12}$ and SmRu$_4$P$_{12}$ at 8K, on the other hand, the Drude component below 0.3eV disappeared and a new band, which corresponds to an interband transition, appeared , respectively, around 0.06eV and 0.025 eV. The effective electron number which contribute to the transition below 0.3 eV was estimated and found to be kept constant at both metallic and insulating phases. This means that the band which the Fermi level crosses underwent a very small amount of energy splitting due to the M-I transition and consequently a new interband transition at 0.4 eV appeared.

References

[1] I.Shirotani *et al.*, J.Phys.Chem.Solids **57**, (1996)211. [2] G.P.Meisner, *et al.*, J.Appl.Phys.**57**, (1985)3073.
[3]C.Sekine, T.Uchiumi, I.Shirotani, and T.Yagi, Phys.Rev.Lett.**79**, (1997)3218.

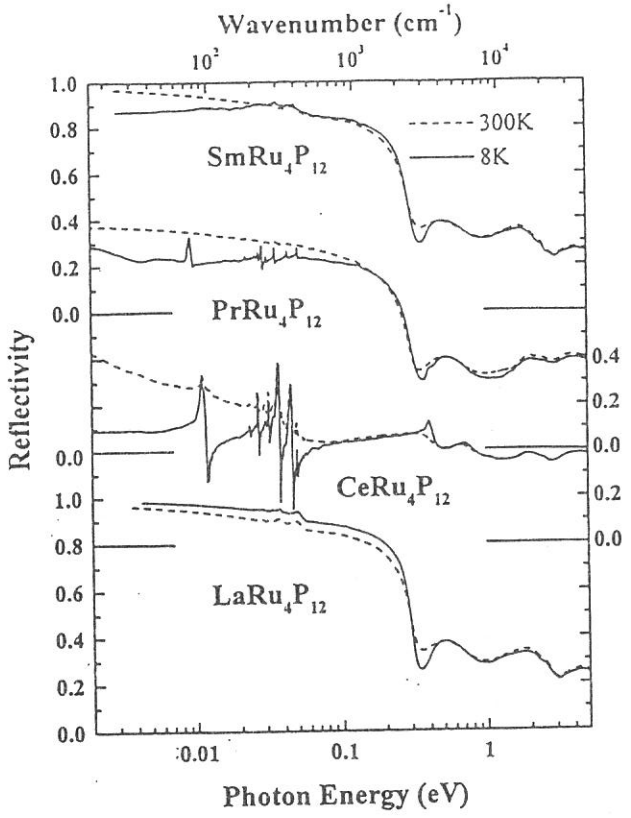

Fig.1

Reflection spectra of RRu$_4$P$_{12}$ (R=La,Ce,Pr and Sm) at 300 K (dashed line) ,78 K(dotted line) , and 10 K (solid line).

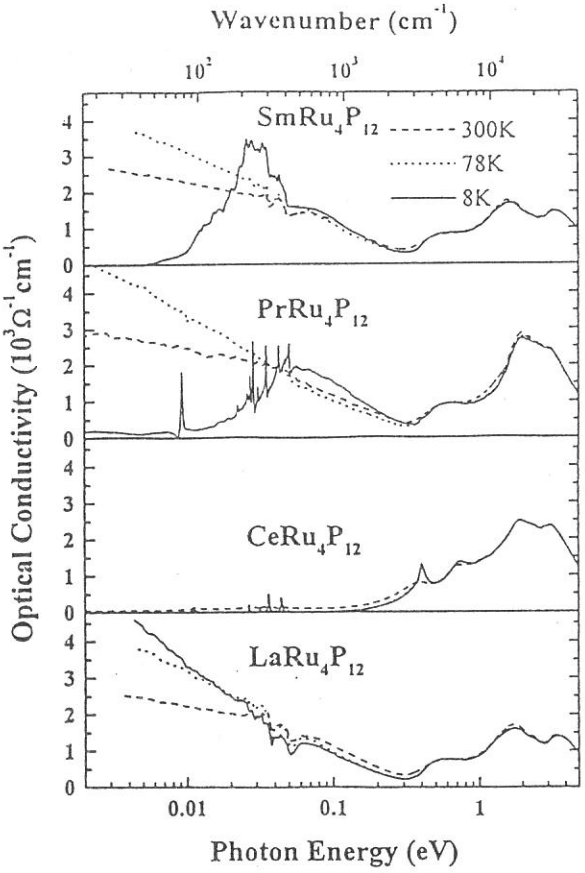

Fig.2 σ spectra of PrRu$_4$P$_{12}$ of RRu$_4$P$_{12}$ (R=La,Ce,Pr and Sm).

(BL6A1)

Infrared Magnetic Linear Dichroism of CeSb

Mitsuru Okuno[1], Shin-ichi Kimura[1,2], Hideaki Kitazawa[3], Giyu Kido[3], and Takashi Suzuki[3]

[1]*Graduate School of Science and Technology, Kobe University, Nada-ku, Kobe 657-8501*
[2]*PRESTO, Japan Science and Technology Corporation*
[3]*Physical Properties Division, National Research Institute for Metals, 1-2-1 Sengen, Tsukuba, 305-0047*

When magnetic field is applied to a material, the physical properties parallel and perpendicular to the magnetic field become different from each other. For instance, the anisotropy has been observed in electrical resistivity[1] and de Haas van Alphen experiments[2] and so on. The anisotropy originates from the electronic structure near the Fermi level. Here, the investigation of the anisotropic electronic structure is main theme.

We have started reflectivity measurement using linear polarized infrared synchrotron radiation which electric vector was set parallel ($\boldsymbol{E}$ // $\boldsymbol{H}$) and perpendicular ($\boldsymbol{E} \perp \boldsymbol{H}$) to an applied magnetic field (infrared magnetic linear dichroism, IRMLD). In our previous experiment of magnetic circular dichroism in infrared region (IRMCD), the light is irradiated from the same direction of magnetic field, *i.e.*, the electric vectors with right and left circularly polarizations is perpendicular to the magnetic field. Then the spectrum of $\boldsymbol{E} \perp \boldsymbol{H}$ is equal to the average of the spectra with both circularly polarizations, on the contrary, the spectrum of $\boldsymbol{E}$ // $\boldsymbol{H}$ provides us new information of electronic structure along the magnetic field. For instance of the AFP1-phase of CeSb, the configuration of magnetic structure, applied magnetic field and electric vector are shown in Fig. 1. In CeSb, magnetic layers are stacked along the magnetic field like a sandwich. In the AFP1-phase case, the magnetic structure has the wave number of k = 2/3, *i.e.*, the periodic magnetic structure with three layers (+ 0 −) appears. Here, + and − indicate the direction of the

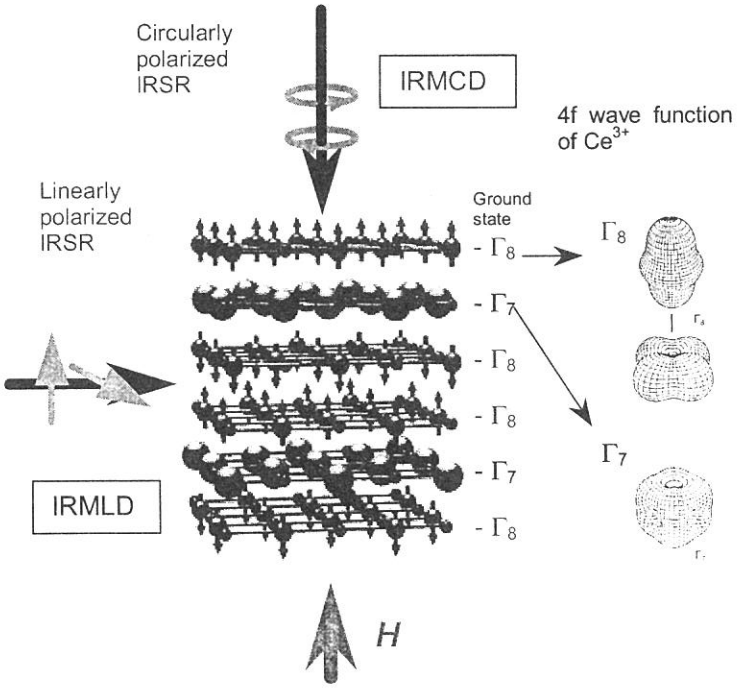

Fig. 1. Magnetic structure in AFP1-phase of CeSb and layered structure of Ce^{3+} 4*f* ground state of Γ_7 (largest sphere) and Γ_8 (middle-size sphere with an arrow). Smallest sphere indicates Sb-ion. Arrows indicate applied magnetic field, incident lights and electric vectors. Configurations of infrared magnetic circular dichroism (MCD) and infrared magnetic linear dichroism (IRMLD) experiments are also depicted.

magnetic moments of Ce $4f$ Γ_8 state and 0 the Ce 4f Γ_7 state. The IRMCD spectrum, as well as the spectrum of $\boldsymbol{E} \perp \boldsymbol{H}$, reflects the electronic structure along the layer of the sandwich structure. The spectrum of $\boldsymbol{E} // \boldsymbol{H}$ only detects the electronic structure along the magnetic field.

We measured the IRMLD spectra of CeSb. The material shows anomalous magnetic phase diagram and also magnetic structure as described in a previous report.[3] Here, we cleaved along the (100)-plane to obtain the clean surface and set the [001] direction parallel to the magnetic field. The light was irradiated from the [100] direction and the electric vector was parallel and perpendicular to the [001] direction.

The reflectivity spectra in some magnetic phases of CeSb with the configurations of $\boldsymbol{E} // \boldsymbol{H} //$ [001] and $\boldsymbol{E} \perp \boldsymbol{H} //$ [001] are shown in Fig. 2. The legends of the magnetic phase have the same notations as those of neutron scattering.[4] In the AF-, AFPx- (x = 1 ~ 5) and P-phase, the spectra in two configurations are similar to each other. However, the spectra are different in the F-, FPx- and AFFx-phase. This indicates that the electronic structure has strong anisotropy due to the different Ce^{3+} $4f$ Γ_8 ground state and the periodic structure.

---

[1] Ex.) T. Terashima, J.S. Qualls, T. F. Stalcup, J. S. Brooks, H. Aoki, Y. Haga, A. Uesawa and T. Suzuki, Phys. Rev. B **60**, 15285 (1999).

[2] Ex.) H. Kitazawa, Y. S. Kwon, A. Oyamada, N. Takeda, H. Suzuki, S. Sakatsume, T. Satoh, T. Suzuki and T. Kasuya, J. Magn. Magn. Mater. **76-77**, 40 (1988).

[3] S. Kimura, H. Kitazawa, G. Kido and T. Suzuki, UVSOR Activity Report 1998, 160 (1999); J. Phys. Soc. Jpn. **69** (2000) in press.

[4] J. Rossat-Mignod *et al.*, J. Magn. Magn. Mater. **52**, 111 (1985).

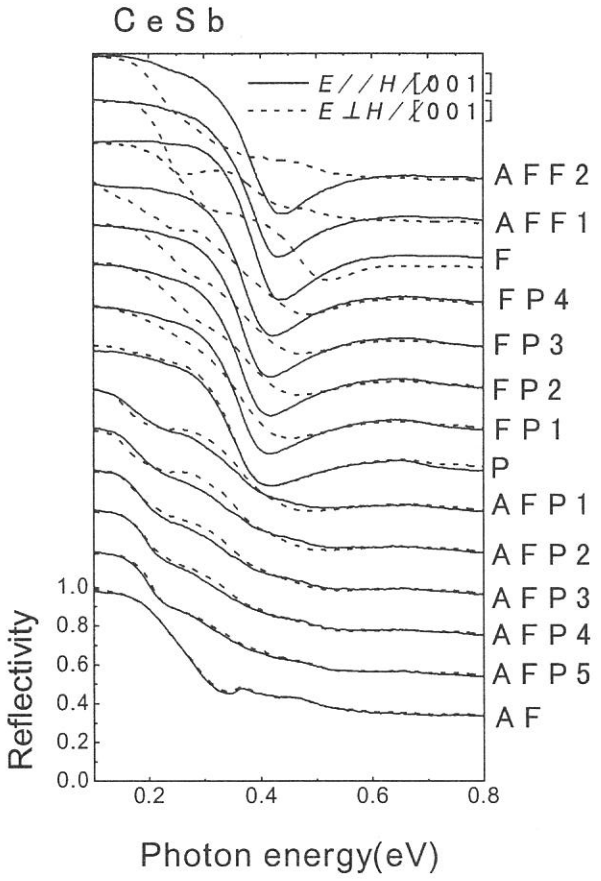

Fig. 2. Reflectivity spectra in some magnetic phases of CeSb with the configurations of $\boldsymbol{E} // \boldsymbol{H} //$ [001] and $\boldsymbol{E} \perp \boldsymbol{H} //$ [001]. The legends have the same notation as those of neutron scattering. Successive curves are offset by 0.2 for clarity.

(BL6A1)

Low Energy Electronic Structure of $Yb_4(As_{0.85}P_{0.15})_3$

Shin-ichi Kimura[1], Mitsuru Okuno[1], Hidekazu Aoki[2] and Akira Ochiai[2]

[1]*Graduate School of Science and Technology, Kobe University, Nada-ku, Kobe 657-8501*
[2]*Department of Material Science and Technology, Niigata University, Niigata 950-2181*

In Yb_4As_3, the relation between transport and magnetic properties is open to question because there is no relation between them at first sight. The magnetic susceptibility does not change in spite that the carrier density is controlled by the substitution of Sb and P for As.[1,2] Then we consider the key to solve the contradiction, we are investigating the electronic structure near the Fermi level using a reflectivity measurement in the infrared region.

In Yb_4As_3, the optical conductivity indicates the transport property continuously changes from the high carrier density and the short relaxation time above 200 K to the low carrier density and very long relaxation time below 100K.[3] The origin of the carriers at high temperature is considered to originate from the Yb 4*f* state because the state crosses the Fermi level observed by a photoemission experiment.[4] However, the origin of carrier at low temperature is still unresolved.

We have investigated the temperature dependence of the electronic structure very near the Fermi level as well as that of the carrier character at low temperature of Yb_4As_3 using far-infrared reflectivity measurement.[5] At the result, we found a new absorption peak at 30 meV and it becomes sharp coincident with the growing-up of the Drude-like carrier absorption with decreasing temperature. To clarify the origin of the absorption at 30 meV, we measured far-infrared reflectivity spectra of a semiconducting material $Yb_4(As_{0.85}P_{0.15})_3$ with a tiny energy gap.

Figure 1 indicates the temperature dependence of optical conductivity ($\sigma(\omega)$) spectra, which are derived from the Kramers-Kronig analysis of the reflectivity spectra of $Yb_4(As_{0.85}P_{0.15})_3$. We are not concerned with some peaks of 10 – 35 meV here because they originate from TO-phonons. The temperature dependence below 0.6 eV is strong. However, the temperature dependence is almost linearly, *i.e.*, the metallic $\sigma(\omega)$ spectrum simply changes into the semiconducting with decreasing temperature. This is not equal to the situation of Yb_4As_3, in which another Drude-like carrier absorption appears at low temperature and also an absorption peak at 30 meV appears. This result means that the absorption peak at 30 meV of Yb_4As_3 is accompanied with the Drude-like absorption at low temperature. Therefore it is considered that the carriers at low temperature originate from the quasiparticle after hybridization between As-4*p* and Yb-4*f* states and the absorption between the hybridization gap appears at 30 meV.

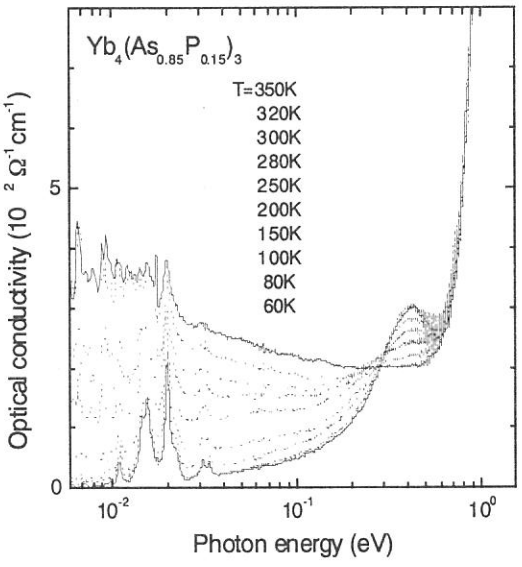

Fig. 1. Temperature dependence of optical conductivity spectrum of $Yb_4(As_{0.85}P_{0.15})_3$ in the infrared region.

[1] H. Aoki, A. Ochiai, T. Suzuki, R. Helfrich and F. Steglich, Physica B **230-232** (1997) 698.
[2] A. Ochiai, H. Aoki, T. Suzuki, R. Helfrich and F. Steglich, Physica B **230-232** (1997) 708.
[3] S. Kimura, M. Ikezawa, A. Ochiai and T. Suzuki, J. Phys. Soc. Jpn. **65** (1996) 3591.
[4] S. Suga *et al.*, J. Phys. Soc. Jpn. **67** (1998) 3552.
[5] S. Kimura, A. Ochiai and T. Suzuki, UVSOR Activity Report 1997 (1998) 124.

(BL7A) Temperature dependence of AlN reflectivity in VUV region

Q.X. Guo[1], A. Okada[1], M. Nishio[1], H. Ogawa[1], K. Fukui[2], H. Miura[3], and A. Yoshida[4]

[1]*Department of Electrical and Electronic Engineering, Saga University, Saga 840-8502*

[2]*Institute for Molecular Science, Okazaki, 444-8585*

[3]*Department of Electrical and Electronic Engineering, Fukui University, Fukui 910-8507*

[4]*Department of Electrical and Electronic Engineering, Toyohashi University of Technology, Toyohashi 441-8580*

Aluminum nitride (AlN), one of the III-V compound semiconductors with a wurtzite crystalline structure, is promising not only for the use of passivation of semiconductor surfaces and insulators for high temperatures, but also for the use of optical devices at ultraviolet spectral region and surface acoustic wave devices, because it has wide band gap and high sound velocity. Recently, it has received more attention from the properties of its alloys with GaN and InN which permit the fabrication of AlGaInN based shortest-wavelength semiconductor laser diode. In spite of the prospects of AlN in device applications, experimental data on the optical properties are surprisingly scarce, although several theoretical studies were performed. We have reported reflectance spectra measured with synchrotron radiation on AlN single crystals in the energy from 6 to 120 eV at room temperature [1,2]. In this work, we investigated the temperature effect on the reflectance spectra of AlN single crystal.

AlN films were grown epitaxially on (0001) α -Al_2O_3 substrates using the chemical reaction of trimethylaluminum with ammonia [3]. Reflection high-energy electron diffraction results showed all the AlN samples to be a single crystal and to have an orientation relationship of (0001)AlN//(0001) α -Al_2O_3. The samples were placed in a continuous-flow cryostat with a coolant (liquid helium) from a storage vessel to a vacuum-insulated sample space. The sample temperature could be maintained at any temperature with an accuracy of 0.1 K in the range of 4.2 to 300 K by controlling the flow of the coolant and the power supplied to the electrical heater. Reflectance spectra were measured in the photon energy range from 6 to 10 eV as a function of temperature. The results show that with decreasing temperature, the energy positions of the dominant structures in the reflectance spectra shift towards higher energies. The shifts of these dominant structures can be well described by the Bose-Einstein expression and the calculated parameters by fitting the experimental data to the expression have a good agreement with those obtained by absorption spectra measurements [4].

The authors would like to thank Professor K. Tsubouchi of the Research Institute of Electrical Communication, Tohoko University, for supplying the samples of AlN single crystal.

References:

[1]Q.X. Guo, M. Nishio, H. Ogawa, and A. Yoshida, Phys. Rev. B 55, R15987 (1997).

[2]Q.X. Guo, M. Nishio, H. Ogawa, and A. Yoshida, J. Crystal Growth 189/190, 457 (1998).

[3]M. Morita, N. Uesugi, S. Isogai, K. Tsubouchi, and N. Mikoshiba, Jpn. J. Appl. Phys. 20, 17 (1981).

[4]Q.X. Guo and A. Yoshida, Jpn. J. Appl. Phys. 33, 2453 (1994).

(BL7B)

Optical reflectivity study of $(Fe_{1-x}V_x)_3Al$ intermetallic alloys

H. Okamura, J. Kawahara, T. Nanba, S. Kimura,
K. Soda[A], U. Mizutani[A], Y. Nishino[B], M. Kato[B]

Department of Physics and Graduate School of Science and Technology, Kobe University, Kobe 657-8501.
[A]Department of Crystalline Materials Science, Nagoya University, Nagoya 464-8603, Japan
[B]Department of Materials Scienceand Engineering, Nagoya Institute of Technology, Nagoya 466-8555, Japan.

The Heusler-type intermetallic compound Fe_2VAl has recently attracted much interest since it possesses several anomalous properties [1]. Fe_2VAl shows semiconductor-like transport data at temperatures above ~ 400 K, but it shows highly metallic photoemission data at low temperatures (40 K). In addition, it shows an anomalous enhancement of specific heat below 4 K, which is reminiscent of typical behaviors shown by the f-electron heavy electron systems [1]. In order to probe the electronic structures of Fe_2VAl and related compounds, we have performed optical reflectivity experiments of $(Fe_{1-x}V_x)_3Al$ ($0 \leqq x \leqq 0.33$) at photon energies between 0.08 eV and 30 eV and at temperatures between 9 K and 300 K [2]. The optical reflectivity spectra above 2 eV were measured at BL7B of UVSOR, while the spectra at lower energy were measured at Kobe University. Figures 1 and 2 show the measured optical reflectivity spectra $R(\omega)$ and the corresponding optical conductivity spectra $\sigma(\omega)$, respectively, measrued at room temperature. $\sigma(\omega)$ were obtained from R (ω) using the Kramers-Kronig relations. With increasing x, $R(\omega)$ shows large decreases below ~ 1 eV, and correspondingly $\sigma(\omega)$ also decreases below 0.5 eV. This demonstrates the formation of a well-developed pseudogap with increasing V content. For the Heusler composition Fe_2VAl (x=0.33), the spectra show only minor temperature dependence down to 9 K [2], showing that the pseudogap results from the band structure of Fe_2VAl rathre than from temperature-sensitive electron correlation effect. Based on the present results, we have proposed a simple model of electronic structures that accounts consistently for both the semiconductor-like transport and the metallic photoemission data of Fe_2VAl [2].

References

[1] Y. Nishino *et al.*, Phys. Rev. Lett. **79**, 1909 (1997).

[2] H. Okamura *et al.*, to appear in Phys. Rev. Lett. (2000).

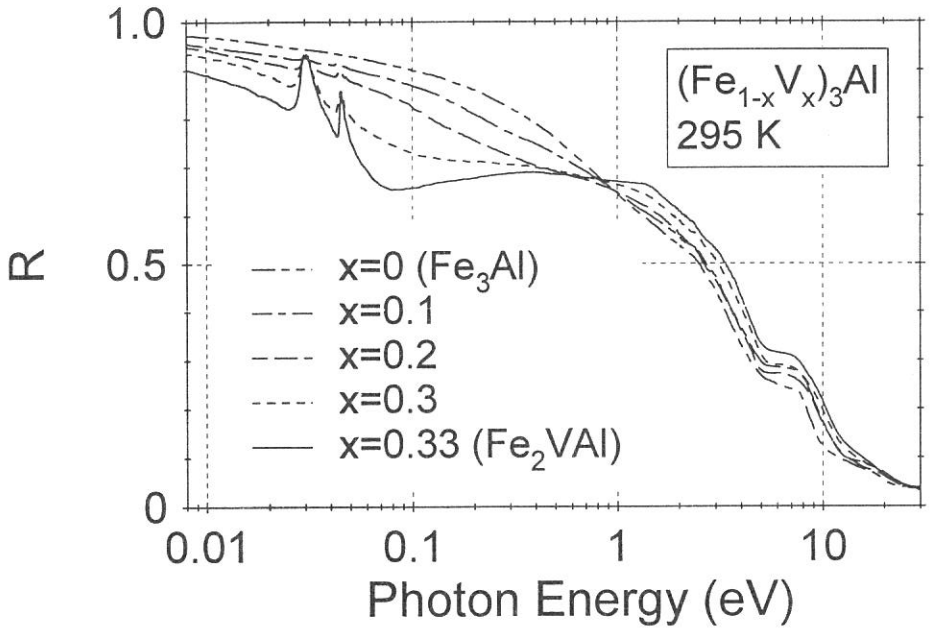

FIG. 1. The optical reflectivity (R) spectra of $(Fe_{1-x}V_x)3Al$ at room temperature.

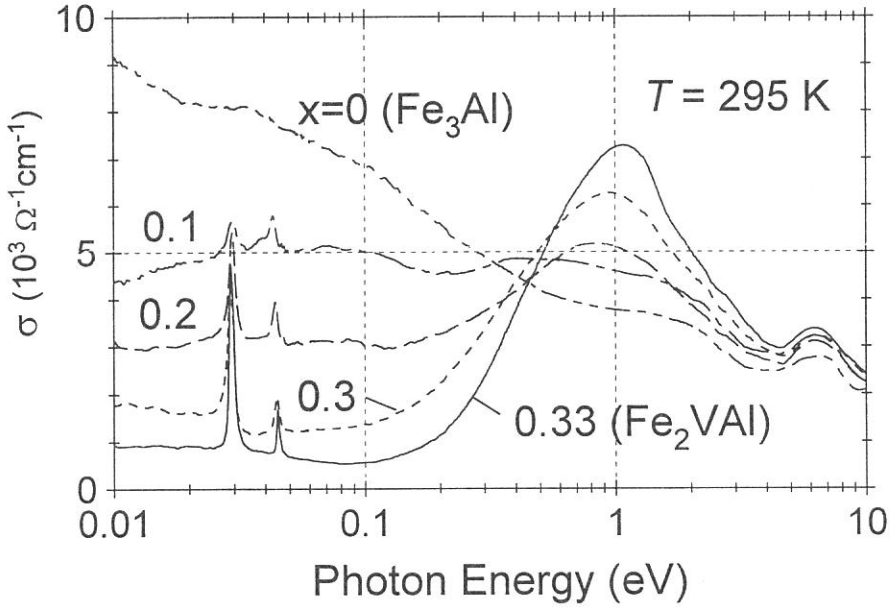

FIG.2 : Optical conductivity (σ) of $(Fe_{1-x}V_x)_3Al$ at room temperature, which are obtained from the spectra in Fig. 1 using the Kramers-Kronig relations.

(BL-7B)

Photo-Dissociation Process of tetraethoxysilane, tetraethoxygermanous and tetraethylsilane induced by Vacuum Ultraviolet Radiation

Hideaki Yanagita, Yasuhiro Kawasaki, Yoshihiro Maesono[a], Ryo Nomura[a],
Noritaka Takezoe, Atsushi Yokotani[a] and Kou Kurosawa

Institute for Molecular Scinece, Myoudaiji, Okazaki 444-8585
[a]Miyazaki University, Miyazaki 889-2192

Tetraethoxysilane (TEOS:Si $(OC_2H_5)_4$) or tetraethoxygermane (TEOG:Ge $(C_2H_5)_4$) is one of the promising materials for preparing SiO_2 or GeO_2. These films have been prepared by photo-chemical vapor deposition using VUV excimer lamp from TEOS or TEOG at room temperature. We have measured absorption spectra of TEOS and TEOG using synchrotron radiation (BL-1B and 7B) with the aim to search suitable wavelength of the light souce for films preparation, and also measured absorption spectrum of tetraethylsilane (TES:Si $(C_2H_5)_4$) which is expected to be a source material for preparing amorphous-Si and SiO_2 films. We have tried to prepare SiO_2 thin films from TEOS using five diffrent excimer lamps (λ =126 ~ 308nm).

Figures 1, 2 and 3 show absorption spectra of TEOS, TEOG and TES at gas pressure of 50mTorr. In the absorption spectra in the region of 115nm to 300nm, TEOS showed absorption in the region shorter than about 180nm, TEOG and TES showed absorption in the region shorter than 200nm. Figure 4 shows FT-IR spectrum from SiO_2 films prepared with five different excimer lamps. SiO_2 films were deposited in case of using Ar_2^* (126nm), Kr_2^* (146nm) and Xe_2^* (172nm), but not with KrCl* (222nm) and XeCl* (308nm), which is consistent with the absorption spectra.

We are planning to investigate photo-dissociation process of TEOS, TEOG and TES with UVSOR by means of mass and FT-IR spectroscopy.

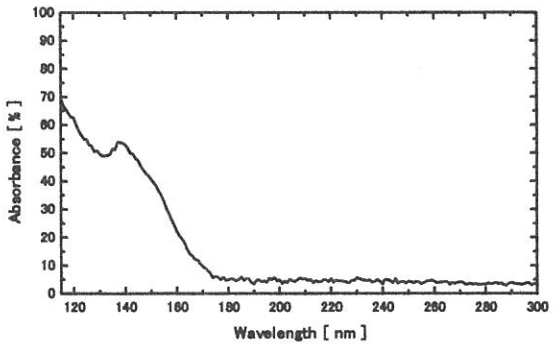

Figure 1 Absorption spectrum of TEOS

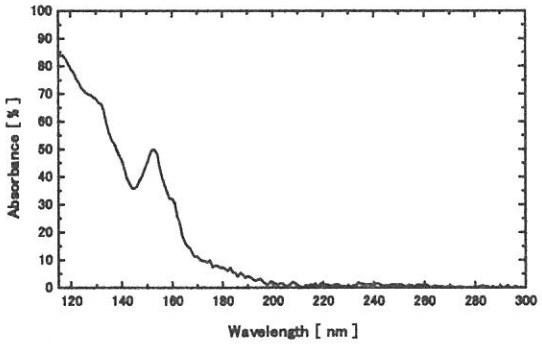

Figure 2 Absorption spectrum of TEOG

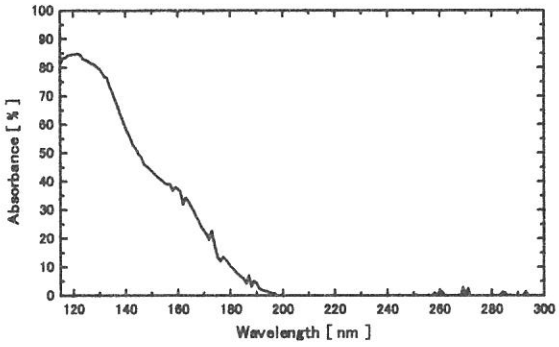

Figure 3 Absorption spectrum of TES

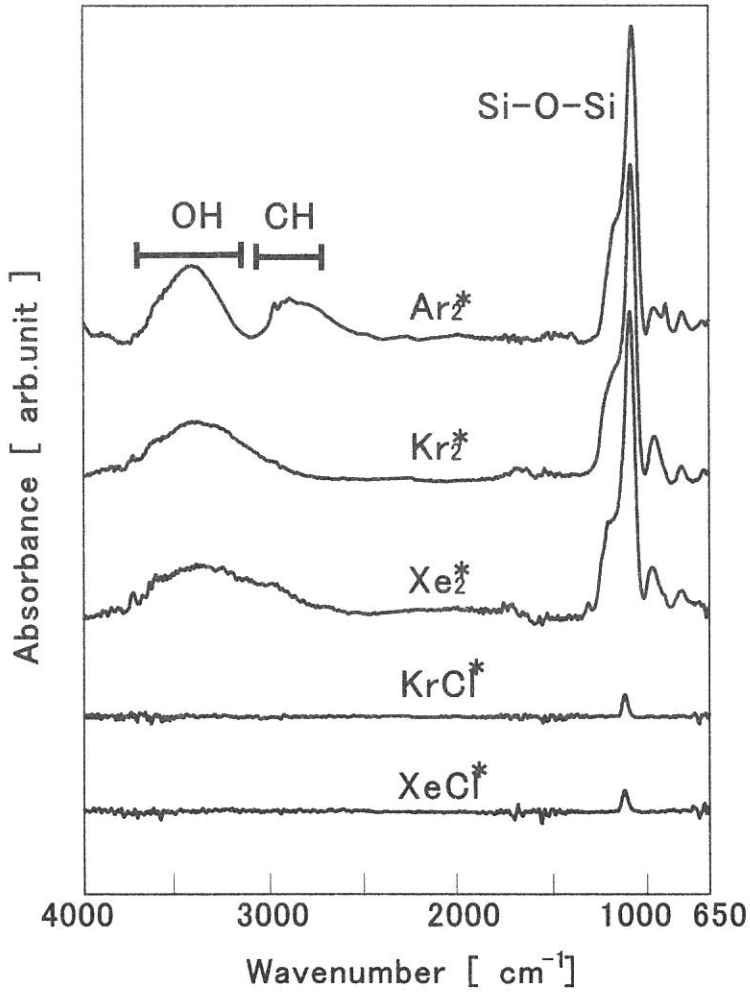

Figure 4 FT-IR spectra from SiO_2 films prepared with five different excimer lamps.

(BL8B2)

Angle-resolved UPS of In/PTCDA interface

K. K. Okudaira, Y. Azuma, S. Akatsuka, Y. Harada[A], and N. Ueno

Graduate School of Science and Technology, Chiba University, Chiba 263-8522
[A]Life Culture Department, Seitoku University, Iwase, Matsudo, 271-8555

The archetypal organic semiconductor, perylene-3,4,9,10-tetracarboxylic dianhydride (PTCDA), has recently gained increasing interest as a promising material for organic electroluminescence devices. It was reported that a thin film of PTCDA provides a new state in the PTCDA band gap due to the reaction between the film and orverlayer materials such as In, Al, Ti, and Sn.[1] This result is very important because the new band is located very close to the Fermi level, and therefore it is expected that it plays an important role in organic devices properties.

In this work, In-PTCDA system was measured by angle-resolved ultraviolet photoelectron spectroscopy (ARUPS) with synchrotron radiation in order to study the origin of the band gap state. We report the results of quantitative analysis of the take-off angel (θ) dependence of the photoelectron intensity from the new band using single-scattering approximation combined with *ab initio* molecular orbital calculation (SS/MO).[2]

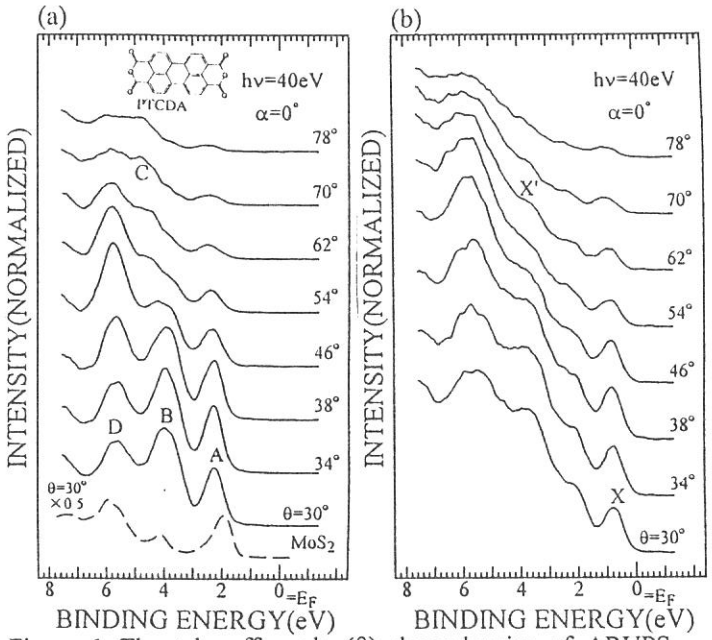

Figure 1 The take-off angle (θ) dependencies of ARUPS spectra of a 3−Å−thick PTCDA film on MoS_2 before (a) and after In overlayer deposition (b). The thickness of the In overlayer is 1Å. The intensity is normalized to the incidence photon flux. The molecular structure of PTCDA is also shown in Fig.1(a).

ARUPS measurements were carried out at the beamline BL8B2 of the UVSOR at the Institute for Molecular Science. ARUPS spectra were measured at photon energy hν=40eV and at incidence angle of photon α=0°. All measurements were carried out at room temperature under UHV conditions (~10^{-10} Torr). Purified PTCDA was evaporated onto a MoS_2 substrate obtained by *in situ* cleavage. The In overlayer was deposited onto the PTCDA film by vacuum evaporation.

In Fig.1(a), we show the θ dependence of the ARUPS of PTCDA thin film (3Å thick; ~monolayer) on the MoS_2 surface, where the binding energy is measured from the Fermi level. These spectra are in good agreement with previously reported results, indicating that PTCDA molecules lie flat on the MoS_2.[3] The assignment for each band in the spectra was already made with *ab initio* calculation and the quantitative analysis of the photoelectron intensity.[3]

Figure 1(b) shows the θ dependence of the ARUPS of an In/PTCDA interface which was prepared by evaporating the In onto the 3-Å-thick PTCDA film. The thickness of the In overlayer was 1 Å. From the comparison between Figs.1(a) and 1(b), some spectral changes can be clearly seen. First, a new band X appears at E_B = ~ 0.8eV in the PTCDA band gap after the In deposition. Second, the band C in Fig. 1(a) ($n_{O\parallel}$:oxygen 2p nonbonding states distributed